Review

Contributions of the Swift/UV Optical Telescope to the Study of Short Gamma-ray Bursts

M. De Pasquale

Special Issue

Contributions of the Swift/UV Optical Telescope to the Study of Short Gamma-ray Bursts

M. De Pasquale ⓘ

Department of Mathematics, Informatics, Physics and Earth Sciences, University of Messina,
Viale F. S. D'Alcontres 31, 98166 Messina, Italy; masdepasquale@unime.it

Abstract: Before the Neil Gehrels Swift Observatory, we knew little about short-duration Gamma-ray bursts (sGRBs). Their briefness led to the suspicion that they resulted from mergers of compact objects, e.g., two neutron stars or a neutron star and a black hole. However, proof was lacking. sGRB post-prompt emission, or afterglow, was undetected; thus, we could not apply essential investigation tools. Swift was the first to pinpoint sGRB afterglows. sGRBs were found to differ from long GRBs in terms of host galaxies, offset from host, environment, energy and progenitors. The Swift UV/Optical Telescope (UVOT) has greatly contributed to these discoveries with its unique combination of fast repointing capabilities and UV sensitivity. But the long-sought proof of the sGRB–merger connection arrived in 2017. The gravitational signal GW 170817A caused by two NSs collision was associated with sGRB 170817A. Swift/UVOT discovered that its early optical emission was—unusually for GRB afterglows—thermal. It was interpreted as an emission from the merger's hot debris: the kilonova. Kilonovae have seemingly been found in other sGRBs and—puzzlingly—in long GRBs. Over almost 20 years, Swift/UVOT observations have also been pivotal to understanding peculiar events. In this review, I will summarize UVOT's major contributions in the fields highlighted.

Keywords: Gamma-ray bursts; gravitational waves; afterglows; compact objects

1. Introduction

Gamma-ray bursts (GRBs) are evanescent, high-energy (X-ray and γ-ray) sky transients [1]. They are observed with a random position and occur about once a day. Briefly, they are the most luminous sources of energy in the Universe, reaching up to $\sim 10^{53}$ erg s^{-1} assuming isotropy. Thanks to the large number of statistics built by the BATSE instrument onboard the Compton Gamma-ray Observatory (CGRO, [2]), it has been known since 1993 [3] that GRBs form two distinct groups. One typically has a high energy and "prompt" emission duration of less than ~ 2 s, whereas the other group is generally formed by events longer than ~ 2 s[1]. The nicknames of such GRBs are "short" and "long" GRBs, respectively. The spectra of the sources of the two classes differ as well: while the short GRBs are often hard, the long ones are usually soft. Clearly, the 2 s divide is rather artificial; diverse instruments will have different sensitivity in different parts of the spectrum and may set the divide at a different time [4]. Despite these issues, the presence of two classes of events was proven beyond doubt.

The extragalactic nature of long GRBs was determined thanks to the Italian–Dutch satellite BeppoSAX [5,6] in 1997. Its X-ray wide field cameras pinpointed the prompt emission and allowed narrow field instruments to find the so-called "afterglow" emission, coming after the prompt, which in turn enabled us to find GRBs' redshifts, energies, ejecta geometries, radiation mechanisms and host galaxies [7,8].

As for the origin of long GRBs, it was found in 1998, when they were first associated with a peculiar class of energetic Type Ic supernovae (GRB-SNe; [9]) and correlated well with the star-forming regions in star-forming galaxies [10,11]. Successively, investigated

nearby long GRBs have shown features due to Type Ic SNe in their light-curve and spectra. Such associations have been ultimately possible thanks to the well-localized GRB afterglows.

The origin of the short GRBs (sGRBs), with duration of $\sim$2 s or much less, remained obscure for longer. They did not produce a detection in BeppoSAX wide field cameras or in general X-ray detectors in space, nor an afterglow in telescopes when these were repointed to the direction of the burst, hours or even days after the trigger. Still, their brief duration suggested a scenario involving two compact objects, for example, a binary system of two neutron stars (NSs) or an NS and a black hole (BH). They would spiral in, losing energy via gravitational waves (GWs). Eventually, the two objects would merge at a fraction of the speed of light in an utterly catastrophic event in which the laws of physics are pushed to the extreme, generating the short GRB [12,13].

Launched in 2004, the Neil Gehrels [14] Swift Observatory has tremendously advanced our knowledge on sGRBs thanks to the fact that it discovers, localizes with an accuracy of at least a few arcminutes with its Burst Alert Telescope (BAT; [15]), and autonomously starts observations of the newly found GRB with its X-ray [16] and UV/Optical Telescope [17]—XRT and UVOT, respectively—just $\sim$100 s after the trigger. Meanwhile, it notifies ground telescopes of the new source in real time. Crucially, BAT is sensitive enough and it has the accuracy to discover and pinpoint short GRBs, which thus can be immediately (when they are brighter) followed up by other spacecraft instruments and ground observatories. Nowadays, Swift has the only fast re-pointing UV observatory in space, with sensitivity between 170 and 650 nm. Its first detection of optical emission from a GRB is that of the long GRB 050318 [18]; the first sGRB with optical afterglow detected by UVOT is sGRB 060313 [19]. Since then, Swift has allowed us to individually and systematically study the sGRB's weak X-ray and optical afterglows [20,21] from the very beginning. Swift was the first mission to find the host galaxy of a sGRB (sGRB 050509, [22]), which turned out to be a passive (i.e., without present star formation) galaxy, and enabled us to determine other associations between a non-star-forming galaxy and a short burst, to unearth sGRBs redshifts, to find large off-sets of sGRBs from their hosts, to constrain a low density for sGRB surroundings [23–25], and to determine the absence of any supernova associated down to very deep upper limits [10,26]. All these findings converged to or were at least consistent with the merger scenario. However, the "smoking gun" for the sGRB progenitor had not yet been found.

Finally, in 2017, the watershed event happened. The Advanced LIGO telescope [27] detected GWs from a two-NS merger in a sky area where the Fermi Gamma-ray Burst Monitor (GBM; [28]) simultaneously detected the weak sGRB 170817A [29]. The worldwide hunt for the electromagnetic (EM) counterpart of this event led to the discovery of the uncatalogued optical transient AT2017gfo [30] in the error region. Swift rapidly slewed to study its EM emission with UVOT, and found that the UV-bright AT2017gfo did not show the typical power-law spectrum of GRB afterglows, but it had a rapidly cooling thermal spectrum [31]. The consensus is that AT2017gfo was a kilonova (KN): a theoretically predicted [32] short-duration source appearing early, broadly isotropic, optically thick, and heated by the radioactive decay of the neutron-rich material coming from the impact [32,33]. Spectral analysis has indicated the presence of r-elements (see Section 2.5), confirming the theories that these mergers produce the heaviest neutron-rich nuclei in the Universe. However, AT2017gfo's fast change in colour tells us that the properties of the merger ejecta are not that simple. Given the interest in compact objects such as NS and BH for estimating how much and when the KNe could produce the amount of r-elements in the Universe, and the opportunity to study GWs and physics theories at the extreme, searches for KNe possibly present in other sGRB light curves which are not recognized for what they were have been undertaken. In addition, these searches have also attempted to constrain the dynamics and the temperature/opacity of the kilonova, which can tell us about the physics and the geometry of the merger and its complex outcome. All in all, a new multi-messenger research approach was born in 2017: it attempts to explore

extreme objects and events and their physics by using the two channels of EM and GW radiation. Radio observations showed an off-axis relativistic jet in sGRB 170817A; thus, the low fluence and the late appearance of the "genuine" power-law afterglow emission could be explained as an off-axis point of view ([34,35]; see Sections 2 and 3). Moreover, Swift data have somehow "blurred" the separation between short and long GRBs (see Section 2.7): some short bursts present a spectrally soft "extended emission" (EE) after the initial short spike [36,37], which may cause them to be mistaken for long GRBs if bright enough ([38]; see Section 3).

The Swift UV Optical Telescope has also contributed to the study of several peculiar short GRB afterglows, as in the case of sGRB 090510 and sGRB 060614, by creating early spectra and light curves. While the former is the only short event with Fermi-LAT GeV and simultaneous Swift BAT, XRT and UVOT detection, the latter is a prototype of a "hybrid" class: GRBs that show some characteristics of the short class and of the long class. By unveiling the optical behavior of bursts at the very beginning, UVOT has also enabled us to extend the study of GRB spectra, including sGRB spectra, down to the eV range by building spectral energy distributions that extend over several orders of magnitude and test the models quite strongly.

In this short review, I will thus focus on contributions that UV/Optical Telescope onboard Swift has made to the field of short GRBs.

2. Methods and Results of the Study of Short GRB

2.1. The Swift UV/Optical Telescope

For the particular aim of this article, a brief description of the Swift UV/Optical Telescope and its capabilities is provided. The telescope has a modified Ritchey–Chrétien configuration, with a 30 cm primary mirror and a focal ratio of 12.7. The light that enters the telescope tube is directed by a mirror to the detector behind a filter wheel with 11 positions. There are astronomical band filters, which are *v*, *b*, *u*, *uw*1, *um*2, and *uw*2, in order of decreasing wavelength they let pass; there are also a clear or "white" filter, two grism filters (one for the optical band and one for the UV wavelengths), and a blocked filter. The detector is a charged coupled device (CCD), provided with a mechanism of intensification of the signal. The detector and filter wheel are duplicated for redundancy. The working wavelength band is about 170–650 nm and the field of view is 17′ × 17′, aligned with that of the X-ray telescope that is also mounted on the same optical bench. The CCD has 256 × 256 pixels, but it samples at 2048 × 2048 "virtual pixels" with a resulting point spread function of 0.9″ FWHM. Operating from space where the light background level is much smaller than those at the ground, the UVOT sensitivity was found to be *b*∼22 magnitude source with a 1000 s integration time [39–42].

From the point of view of operation, the UVOT starts observations with a chosen filter when Swift is still slewing but is within 10′ of the target position provided by BAT and XRT. This is the "settling" exposure. Once the spacecraft has stopped slewing, UVOT commences a sequence of exposures that can be modified. The first settled observation provides the "finding chart", whose central part is immediately sent to ground observatories via Notices. UVOT has an catalogue of bright sources in its onboard computer, and it compares the finding chart with the catalogue in the region observed; if a new source is found, this is also stated in the Notices. Typically, the finding chart is taken starting ∼100 s from the burst trigger time given by the BAT [41,42]. Later, the complete finding chart and following observations are downloaded when Swift passes over ground stations.

Overall, with its characteristics, the UVOT has routinely shown us the previously largely unknown initial optical emission of GRB afterglows. Since afterglow emission decays with time, UVOT generally observes it when it is at its brightest and with the best S/N. The capability of starting observations of GRBs that early is of particular importance for sGRBs, given the fact that their afterglows, including optical afterglows, are on average weaker than those of long GRBs ([20]; see also Section 2.2). Moreover, early exposures enable us to study physical processes that are expected to occur in the first few hundred

seconds from the GRB explosion, such as the so-called "reverse shock" and the "forward shock" peaks [43]. Usually, for an afterglow of average brightness, the UV/optical light curve is at least a few hundred seconds long. Other scientific goals of UVOT have been to determine the fraction of bursts that are highly extinguished, the kind of extinction law in far-away galaxies, and, for very bright GRBs, a direct estimate of the redshift thanks to photometry and grisms.

2.2. Short GRBs Observations and Their Physical Parameters

By their very nature, sGRBs are first detected by space facilities because our atmosphere stops the initial X and γ-ray radiation. When a detection is made, follow-up observations take place. Swift BAT operates between 15 and 350 keV and, as already mentioned in the Introduction, is responsible for the discovery and real-time positioning of a high-energy uncatalogued source. This is used by the satellite to autonomously slew and start observations with the XRT and UVOT, usually within $\sim$100 s from the high-energy trigger; XRT and UVOT can also pinpoint the afterglow down to $\sim$1–2". The position is immediately sent to ground observatories. Swift detects about 10 short GRBs/yr, and of these, 7 are immediately localized within a few arcseconds thanks to the detection and localization of their X-ray afterglows by the XRT and sometimes by UVOT (in which case, the localization has $\simeq$0.6" accuracy).

The study of the GRB afterglow is of particular importance because it enables us to test and use the successful "forward shock" model (FS; [21,44]) to study these extremely violent explosions. Basically, it is assumed that the ultra-relativistic ejecta drive a "forward shock wave" ahead of them, thus accelerating electrons of the circumburst medium. In turn, electrons re-emit the acquired energy as synchrotron radiation. With the FS model, one can constrain essential parameters of the burst, such as the opening angle of the outflow and thus the true, beamed-corrected energy, both of which depend on the burst "central engine". Moreover, other shock parameters, such as the fraction of shock energy given to the synchrotron-radiating electrons and to the magnetic field of the circumburst-shocked medium, ϵ_e and ϵ_B, respectively, the index of the power-law energy distribution of radiating electrons p, and the density n of the medium environment itself, can be constrained. However, to use the FS model, one should determine at least the power-law temporal decay and spectral indexes of the afterglows, α and β, respectively, preferably in more than one band. The FS flux density is characteristically a power law both in the space and temporal domain, i.e., $F_\nu \propto \nu^{-\beta} t^{-\alpha}$.

Fong et al., 2015 ([24]; F15 onwards) systematically analyzed the X-ray, optical and radio data of a sample of 107 sGRBs with $T_{90} < 2$ s detected in large majority by Swift (with smaller addition from other orbital facilities) between 2004 and 2015 (a span of about 10 years). The archive they built and the related sources are available in their online article. When taking out those events affected by observational constraints and considering the fact that some events were observed by more than one facility, F15 found that 91% of short GRBs have an X-ray afterglow, 40% have an optical afterglow and 7% have a radio one. The rate of optical detection is essentially the same as that found in the second catalogue of Swift/UVOT GRB afterglows [42], for which detection at $\gtrsim 3\sigma$ level are $\simeq$40% of the total, if one optimally sums the available exposures (for details, see said catalogue). In F15, the X-ray decay index was calculated with a fit based on χ^2 statistics, as in the case of the decay index of the optical emission obtained by one or more good-quality light curves. The decay index α_{opt} thus calculated is used to extrapolate the flux in other filters to a common epoch, thus enabling us to calculate the spectral index β_{opt}. UVOT data were used for this effort essentially in collaboration with ground observatories, since UVOT discovers optical/UV afterglows at the beginning of observations of a newly discovered GRB in $\approx$10% of cases (based on [23] and Oates S., priv. comm.; as mentioned, this fraction rises to $\sim$40% if we include all the UVOT exposures optimally summed together, but temporal information is basically lost in these cases) and UVOT starts taking data very early, giving us leverage to establish the overall light curve. With UVOT, observations at late epochs

have exposures longer than the first, thus allowing us to recover the optical afterglow emission down to a magnitude $b \sim 22$.

F15 analyzed the 38 bursts with the best optical and X-ray data, by means of the equations of the FS model. They fixed $\epsilon_e = \epsilon_B = 0.1$ as fiducial values. However, given the inclusion of radio data, sGRB 050724 and sGRB 140903A require ϵ_B equals to $\lesssim 10^{-4}$, $\lesssim 10^{-3}$, respectively. The fit of sGRB 051221 is significantly better if $\epsilon_B = 0.01$. Furthermore, F15 notes that for 33 bursts out of 38, a solution with $\epsilon_B = 0.01$ is acceptable. F15 then derived how the kinetic energy and density depends on the observed optical, X-ray, and radio (when available) flux density, according to the FS equations. This is because these three bands may be found in three different intervals of the spectrum: between the self-absorption frequency ν_{SA} and the peak frequency ν_M; between ν_M and the cooling frequency ν_C; and above ν_C. Each interval provides a different relation between E and n; thus, for a given flux, it will correspond to a different segment in an $E_K - n$ diagram. The "correct" value of kinetic energy and density is found where the segments intersect. In a few cases, we have only observations in one of the three frequency intervals above; for example, we may have that $\nu_M < \nu_{Opt} < \nu_X < \nu_C$. If radio observations are not available, the two segments corresponding to the optical and X-ray flux have the same slope, they may overlap, and the $E_K - n$ measurement is much less defined and density could take infinitely small values. In practice, we bind n to be $> 10^{-6}$ cm^{-3}. Since E_K and n are inversely proportional, when it comes to produced flux, the low bound for n creates an upper limit of E_K as well. In this sense, one may say that energy and density are somehow degenerated. When radio data are available, even in the form of upper limits, they provide another constraint. Moreover, F15 imposes a further constraint that ν_C, which depends on E_K and n, is higher than $\simeq 2.4 \times 10^{18}$ Hz = 10 keV in the frequency configuration above; the opposite applies if $\nu_C < \nu_X$. Finally, F15 found that having different minimum values of density does not greatly affect the median of the distribution of this parameter. Overall, with the aforementioned values of the ϵ's parameters (and the exceptions for sGRBs 050724 and 140903A), F15 found that the density and isotropic kinetic energy median values are $<n> \simeq 2.9 \times 10^{-3}$ cm^{-3} and $<E_{K,iso}> \simeq 1.9 \times 10^{51}$ erg. The cumulative distribution of density gives $n \lesssim 1$ cm^{-3} in 95% of cases. F15 noted that events with a "high" density may only be found close to their host. Among the 38 events, 18 GRBs have the synchrotron cooling frequency ν_C and injection frequency ν_M in the following order: $\nu_X > \nu_C > \nu_{OPT} > \nu_M$. These events have better-constrained energy and density (one can use two or three equations provided by the FS model, that is, two or three segments of different slopes in the $E_K - n$ diagram). Assuming the aforementioned values for ϵ_B and ϵ_e, F15 found a density median $<n> = 3.7 \times 10^{-2}$ cm^{-2}; 90% of GRBs have $n \lesssim 1$ cm^{-3}. The median kinetic energy assuming isotropy is $<E_{K,iso}> \simeq 9.6 \times 10^{50}$ erg. Finally, even adopting $\epsilon_B = 0.01$ for all bursts except 050724A and 140903A, the median values of kinetic energy and density increase but change by less than a factor of two (Figure 6 of F15).

Surprisingly, for sources often connected with ancient star populations, some short GRBs present significant extinction (~ 1 magnitude). This was taken into account in those bursts with the best data; otherwise, the extinction A_V was fixed to 0. It is remarkable that sGRB 080919 has $A_V \gtrsim 6$ magnitudes (F15).

2.3. Short GRB Host Galaxies

Swift instruments provided the error region of many short bursts that were subsequently investigated by very large telescopes to spot and study the host galaxies, something nearly impossible before. The XRT has a refined error radius of very few arcseconds while, as mentioned, sources in UVOT have positions with less than 1" errors.

In addition, if the sGRB host galaxy was sufficiently close, Swift/UVOT could provide its magnitudes in the UV bands. In doing so, it could help constrain parameters such as the star formation rate (De Pasquale et al.).

Fong et al. (2022) ([25], F22 onwards) analyzed all sGRBs from Swift's launch to 2021 whose positions had an error $\lesssim 5''$ in order to attempt a meaningful association with

their host galaxy (almost all XRT-detected bursts obey such a condition). They used the literature/archival data as well as their own observations carried out with large optical and NIR ground facilities, HST and Spitzer. They gathered both photometric and spectroscopic data. They took out the bursts with observational constraints. Astrometry of the host galaxies was carried out over the well-known catalogues Gaia DR2 [45], Pan-STARRS [46], SDSS DR12 [47], or 2MASS [48]; the centroids of the sources was determined via standard software such as SExtractor and IRAF [49–51]. The positions of afterglows were determined again by means of SExtractor and IRAF. The online version of F22 contains the catalogue of the host and afterglow positions. If they could not access afterglow discovery images, they employed published positions from the literature or GCNs. Overall, their sample is constituted of 90 sGRBs. The probability of a galaxy being associated with a GRB was evaluated as in [11]: basically, the probability of finding a galaxy of a given magnitude at a given radius distance from the given afterglow. While they associate 84 sGRBs with galaxies, actually 50 of these (i.e., 56% of the sample) have a probability only of 2% or less of not being the real host. These tend to have the most luminous host galaxies, lower redshifts, and smaller offsets. Bursts for which the probability of a wrong association is larger than 0.02 are still important, because they would still include progenitors that, for example, have traveled further from their birth site. Thus, F22 included galaxies with a probability of being a false of up to 0.2; one major reason for such a high probability is that sGRB and the putative host may well have a large distance, as mentioned.

To determine the redshift, spectroscopic data were analyzed or, when this was not possible, a photometric evaluation was carried out.

Overall, F22 found a median redshift for the full population of $<z> = 0.64^{+0.83}_{-0.32}$, and $<z> = 0.93^{+1.16}_{-0.46}$ for those objects whose redshift was determined photometrically. The median physical offset of sGRB with respect to their host is $7.72^{+20.91}_{-6.05}$ kpc. This is $\simeq 6$ times the offset of long GRBs from their hosts [52]. The offsets of sGRBs with best and clearest data, when compared to the size of their host galaxies, give a median of $1.45^{+2.57}_{-0.93}$ light radius r_e, which is still $\simeq 2.5$ the value for long GRBs. In addition, F22 found that sGRBs with extended emission are not different from events without in terms of off-set.

Another result of F22 is that sGRB hosts have a median luminosity $<L> \approx 8 \times 10^9$ L$_\odot$; sGRB host galaxies seem to be, on average, more luminous than hosts of long GRBs. The latter show several objects with $L \lesssim 10^9$ L$_\odot$, whereas there are only two sGRB hosts with such low luminosities of up to redshift $z \lesssim 3$ (F22). Yet, the deep photometry performed by F22 would have spotted host galaxies with $L < 10^9$ L$_\odot$, at least up to redshift 1.

Nugent et al. (2022) ([53], N22 hereafter) examined the properties of the stellar populations of the sample of host galaxies of F22 with associated sGRBs by means of the PROSPECTOR [54] code in order to constrain the redshift, if not known already, and the stellar population properties, such as stellar mass, star formation rate, metallicity, and dust attenuation. In turn, such measurements about the star populations could inform us about the progenitor of sGRBs. Their sample is somehow reduced from that of F22 since they require observations in at least three filters.

N22 found a median redshift of GRBs with a spectoscopic redshift $<z>= 0.47^{+0.58}_{-0.26}$. If we add the GRBs with photometrical redshift, we find a median of $z = 0.64$; this is not surprising, since photometric redshift allows us to constrain the redshift of objects at $z > 1$. We find that the average stellar mass is $\log M_*/M_\odot = 9.7^{+0.8}_{-0.7}$, SFR $= 1.4^{+9.4}_{-1.4}$ M$_\odot$/year, $\log Z_*/Z_\odot = -0.4 \pm 0.4$, and $A_V = 0.4^{+0.9}_{-0.4}$ magnitudes. Overall, 84% of sGRBs hosts are star-forming objects, 6% are transitioning to quiescent, and 10% are quiescent. The latter percentage rises to $\approx 40\%$ when one considers hosts at $z \lesssim 0.25$. A similar trend is also found in the general field galaxy population. sGRB hosts populate the star-forming main sequence (SFMS; see, e.g., [55,56]), i.e., the star formation rate as a function of stellar mass. In this case, they behave like most field galaxies (note that SFMS changes with redshift: the higher the redshift, the more star-forming a galaxy is for a given stellar mass). In other words, the hosts of sGRBs have a star formation rate typical of their mass and redshift:

more star formation is present in more massive galaxies. We wrote above that the host galaxies of sGRBs do not seem to be dimmer than $\sim 10^9$ $L_\odot$. However, N22 found also that the fraction of massive host sGRB galaxies is lower than that in the field galaxies; thus, sGRB hosts do not track stellar mass alone (see also some very recent and preliminary work from the N22 group [57]). Since these hosts still follow the SFMS, one concludes that sGRBs trace a combination of star formation and stellar mass. N22 found that for those sGRB hosts at $z > 1$, about 1/3 of the sample, the average age of the population is systematically less than $\approx 20\%$ the age of the Universe at that redshift. Note that at $z \approx 1$, we are quite close to the peak of stellar formation in the Universe. Instead, those hosts at $z < 1$ show a wide span of stellar ages. Another result of N22 is that the metallicity is what we would expect from their stellar mass and star formation: sGRBs do not appear to select galaxies for their metallicity. Note, for example, that NGC 4993, the host of the only sGRB so far associated with a GW signal, has an old stellar population, $\simeq 10$ Gyr and nearly solar metallicity. It is also quiescent, and it is not surprising to find such properties in a low-redshift sGRB host.

According to N22, sGRBs seem to be farther away from their host if the galaxy is not star-forming, $26.1^{+34.3}_{-23.7}$ kpc, than if it is star-forming, $9.0^{+11.6}_{-6.82}$ kpc. Such a difference cancels out, though, if one considers the relative size of the galaxies. Nonetheless, a large offset indicates a longer delay time since the formation of these progenitors. Anyway, no correlation between host galaxy distance and SF rate and optical afterglow luminosity is found.

Finally, hosts of long GRBs have, on average, a mass lower by ~ 1 order of magnitude and a few times higher specific star formation rates than hosts of sGRBs (N22). Instead, the hosts of sGRB have typical mass close to the hosts of supernovae Ia, which are thought to derive from an old population.

2.4. Opening Angle of the Ejecta Jet

Short GRBs, like long GRBs, are expected to be beamed, jetted sources. Because of relativistic beaming, the high-energy prompt emission is basically detected only if $\theta_{obs} < \Gamma^{-1} + \theta_{jet}$, where θ_{obs} is the observing off-axis angle, θ_{jet} is the semi-opening angle of the jet, and Γ is the Lorentz factor of the jet. Now, the relativistic beaming effect brings about the "jet break phenomenon". The jet decelerates by piling up circumburst medium; consequently, its Γ decreases and an increasing fraction of the emitting surface is seen. Once the ejecta have decelerated enough, the observer will detect emission from the "edge" of the jet, beyond which there is no more emitting surface. The light curve will thus show a break to a faster decay: this is the jet break [58]. According to the FS model, the decay slope becomes $\alpha \simeq p$ in all bands above ν_M. Finding the opening angle of the short GRB je**t**s is of the utmost importance if we want to compute the true energy and rate of these events ([59]). The opening angle $\theta_{jet} \propto t_{jet}^{3/8}$, where t_{jet} is the jet break time; thus, the longer the observation, the more probable it is to find the jet break. In the sample of F15, only a few bursts showed jet breaks; the weakness of the events may be responsible, given the low count/rate at the epoch of the possible jet break. To consider wide opening angles, F15 added events with published limits on the opening angle (they were observed for several days and led to $\theta_{jet} \gtrsim 5^0$), and bursts of their own analysis. F15 found opening angles variable between 5 and 25 degrees. If one fixes $\theta_{jet} < 30$ degrees, a median of $<\theta_{jet}> = 16 \pm 10$ degrees is found. This is comparable to the $\theta_{jet} = 13^{+5}_{-9}$ degrees found for long GRBs (see F15 and references therein). With this value of θ_{jet}, the typical beamed-corrected energy is $f_b \simeq \theta_{jet}^2/2 \simeq 0.04^{+0.07}_{-0.03}$ times that inferred in the isotropic case. Thus, the typical beamed-corrected total (kinetic + radiated) energy budget of a short GRB is of the order of 10^{49}–10^{50} erg.

2.5. sGRB 170817A—GW 170817—AT2017gfo

Swift/UVOT provided an important contribution to monitoring the UV Optical NIR emission of this source because it is the only fast-repointing UV observatory in space. UVOT began observation of AT2017gfo, the optical counterpart to GW 170817 found in

the passive galaxy NGC 4993 at 43 Mpc [30], about 0.6 days after the GW signal. UVOT data were reduced and analyzed using standard routines—i.e., NASA ftools especially created for UVOT[2]—and procedures. In the first exposures, UVOT detected a source that was bright, especially in the UV, with magnitude $u = 18.19^{+0.09}_{-0.08}$, $uw1 = 19.46 \pm 0.11$ (AB) [31]. The absolute magnitude of this source in the u band is thus $M_u \simeq -15$. Successive exposures showed that the flux at UV wavelength was decaying faster, whereas the source was almost constant in the optical and near-infrared (see Figure 1).
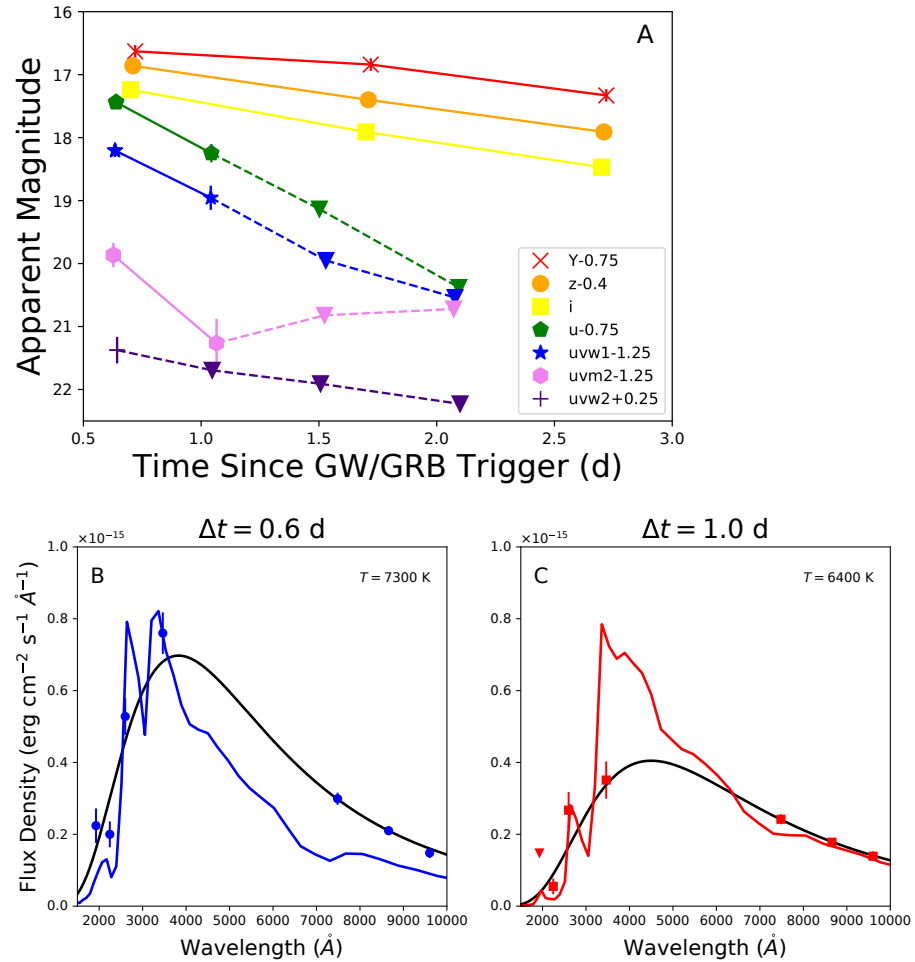

Figure 1. (**A**) Early light curve of AT2017gfo. (**B**,**C**) Spectra of AT2017gfo at 0.6 d and 1 d after Trigger. The blue and red color represent the KN emission at 7300 and 6400 K, respectively. In particular, the "fluctuating" light curves show the observed thermal spectrum after predicted extinction in the source. The non-extinguished spectra show the typical black-body shape. Taken from [31].

The fit of the spectral energy distributions at 0.6 and 1 day after the trigger with a power-law model, which usually reproduces the GRB afterglow spectra, was statistically very poor. Instead, the fit with the thermal spectrum model is good. Moreover, no X-ray emission was detected at the beginning of observations, nor for a few days after the trigger, whereas GRB afterglows are very X-ray luminous after the prompt emission. At 0.6 days, the optical-to-X-ray spectral index limit—built using UVOT data—is $\beta_{OX} > 1.6$, which is hardly found in GRB afterglows. Noticeably, the thermal source was cooling fast. The fitting of the data indicated that the temperatures had decreased from $7300^0 \pm 200^0$ K to $6400^0 \pm 200^0$ K between 0.6 and 1 day. This rapidity excluded a supernova. Furthermore, the thermal emission was also produced by material moving at trans-relativistic speeds. By deriving the radii of the emitting regions at 0.6 and 1.0 days (using the temperature

and the luminosity calculated thanks to knowing the distance) and dividing by the time intervals, one finds speeds of 0.2–0.3 c. This source is the "kilonova".

Several authors investigated how the kilonova source showed a blue component for some time, which points to a low opacity of the emitting medium; then, it turned red, and thus had a high opacity. Ref. [31] tried to recreate the kilonova temporal and spectral behavior as follows. They created several 2D models, varying the parameters of mass, velocity and composition. Two ejecta components were assumed. One is neutron-rich dynamic ejecta, with an electron fraction $Y_e \simeq 0.04$, which produces lanthanides and actinides. These are high-opacity heavy r-elements, where "r" stands for "rapid"; these elements can only form in environments with an extremely large flux of neutrons, with nuclei piling up more neutrons than those that can decay. This is supposed to happen in the "dynamical" ejecta, i.e., matter stripped tidally before the impact or scattered at the moment of impact. The "wind" ejecta instead were given Y_e varying from 0.27 to 0.37 under the assumption that they spent more time close to the neutrino-emitting system formed by a central object and its accretion disk. This object is thought to be a Hyper-Massive Neutron Star (HMNS), or a rapidly rotating black hole ([60]; see Section 3) that formed out of the merger. These ejecta are expected to be less neutron-rich and produce the lightest and most transparent of r-elements. Spatially, the best scenario to explain observations is that dynamical ejecta roughly form a disk around the merged objects; the wind ejecta emerge from the centre of it, possibly helped by the jet that has burrowed a hole through which the wind ejecta can pass. Thus, the light elements are visible only if the off-axis angle is less than 30–40 degrees. This value is in agreement with the GW observations. Moreover, the wind ejecta are taken over by the faster-moving dynamic ejecta within 1–2 days. After some fitting, Ref. [31] find that the UVOIR emission can be globally reproduced with a wind ejecta mass $\gtrsim 0.03\ M_\odot$, $Y_e \simeq 0.27$ and $v = 0.08$ c, while the $Y_e \simeq 0.37$ (Fe-peak elements) is disfavoured. As for the dynamical ejecta, although not well constrained by observations, masses around $0.01\ M_\odot$ and speeds about $v \simeq 0.3$ c give a good fit, in agreement with other studies. A high resolution spectrum of AT2017gfo ([61]; see [62] as well), taken about 1.5 days after the trigger, seems to show spectral features due to the Strontium. This element has an atomic weight of about 90 (there are several isotopes) and atomic number of 38, and is regarded as also being produced in NS mergers as an r-element. Recently, Ref. [63] claimed to have resolved the spectrum of another kilonova, associated with GRB 230307A, and found indication of another r-element, Tellurium, with atomic number Z = 52 and weight ≈130. Note that many neutron-rich r-element nuclei predicted to form in kilonovae are radioactive; this probably contributes to maintaining high the temperature of the ejecta for a relatively long time. All in all, AT2017gfo has demonstrated that NS-NS mergers produce a sizeable amount of r-elements. According to [64], for merger rates consistent with the "best bet" (see Section 3.1), i.e., ∼1000 events $\text{Gpc}^{-3}\ \text{yr}^{-1}$, mergers alone can explain the abundance of r-elements, including the heaviest ones, in the Universe.

An X-ray source at the position of GRB170817A started to be detected $\simeq 9$ days after the trigger by the Chandra X-ray Observatory, and successive Chandra observations showed that this X-ray source brightness was slowly increasing [65]. The detection of the radio counterpart followed two weeks after the trigger [66,67]. In the optical band, one had to wait for the kilonova emission to fade away to find a weak, rising source 110 days after the trigger [68–70]. The spectrum of radio, optical and X-ray emission could be modelled well by a simple power law as predicted by the FS scenario, with $\beta = 0.59 \pm 0.01$. The emission at all wavelengths reached a peak at $\simeq 150$ d and started to decline fast with a decay slope approximately $\propto t^{-2}$, where t is the time since the merging event. A joint fit of all data in several bands (radio, optical, X-ray) with a broken power-law model yields $\alpha_{rise} \approx 0.86 \pm 0.04$, $t_{peak} \approx 155 \pm 0.04$ days, $\alpha_{decay} \approx 1.92 \pm 0.12$ [70,71]. Similar results have been obtained by several authors.

Such an afterglow behavior, though never seen so clearly before, had been predicted for *misaligned jets* (e.g., [72]). At the very beginning, basically all radiation is beamed away from the off-axis observer. As the ejecta and the forward shock producing the emission

slow down, the radiation becomes less and less beamed, until it fully reaches the observer. The maximum occurs when $\Gamma^{-1} \sim \theta_{obs}$, with Γ being the Lorentz factor of the ejecta and θ_{obs} being the angle between the jet axis and the observer. Following this epoch, little and then no illuminating surface enters the line of sight and the light curve begins a steep decay in all bands, typical of a relativistic jet [58] with a decay slope t^{-p}, with $p \approx 2$–2.5 or thereabouts. Note that in this model, the jet must go through and emerge from the merger ejecta and, in doing so, it is likely to acquire a "structure". The core of the jet would have the largest, roughly constant, amount of energy/solid angle, while the "wings" would have less of it. However, the exact structure of the head of the jet is not clear since different models still give acceptable results in reproducing the afterglow rising light curve. Nonetheless, some structure is needed: a "top hat" jet, with uniform energy density throughout the emitting surface, would have shown a much faster rise than that observed [72].

One such model is as follows. By means of fitting multi-wavelength data with the EMCEE Markov Chain Monte Carlo package [73], Ref. [70] assumed that the energy density on the jet head has a Gaussian form, with $E(\theta) = E_0 e^{-\frac{\theta^2}{2\theta_{core}^2}}$. They retrieve a half-opening jet core of $\theta_{core} = 4.50 \pm 0.03$ degrees, a truncation angle (i.e., the half-total angular extension of the jet) $\theta_{wide} = 43.9^{+26.8}_{-21.7}$ degrees, a visual angle $\theta_{obs} = 29.64 \pm 9.12$ degrees, an isotropic kinetic energy $E = (2.95^{+16.10}_{-2.14}) \times 10^{52}$ erg, a beaming-corrected total energy of $E_{tot} = (1.74^{+10.28}_{-1.15}) \times 10^{50}$ erg, environment density $n = 0.015^{+0.073}_{-0.014}$ cm^{-3}, $\epsilon_e = 0.074^{+0.176}_{-0.064}$, $\epsilon_B = (0.66^{+0.42}_{-0.49}) \times 10^{-5}$, $p = 2.17 \pm 0.01$ (see the modeled light curves in Figure 2). The kinetic energy is not subpar when compared to that of other sGRBs. Other authors have obtained similar results.
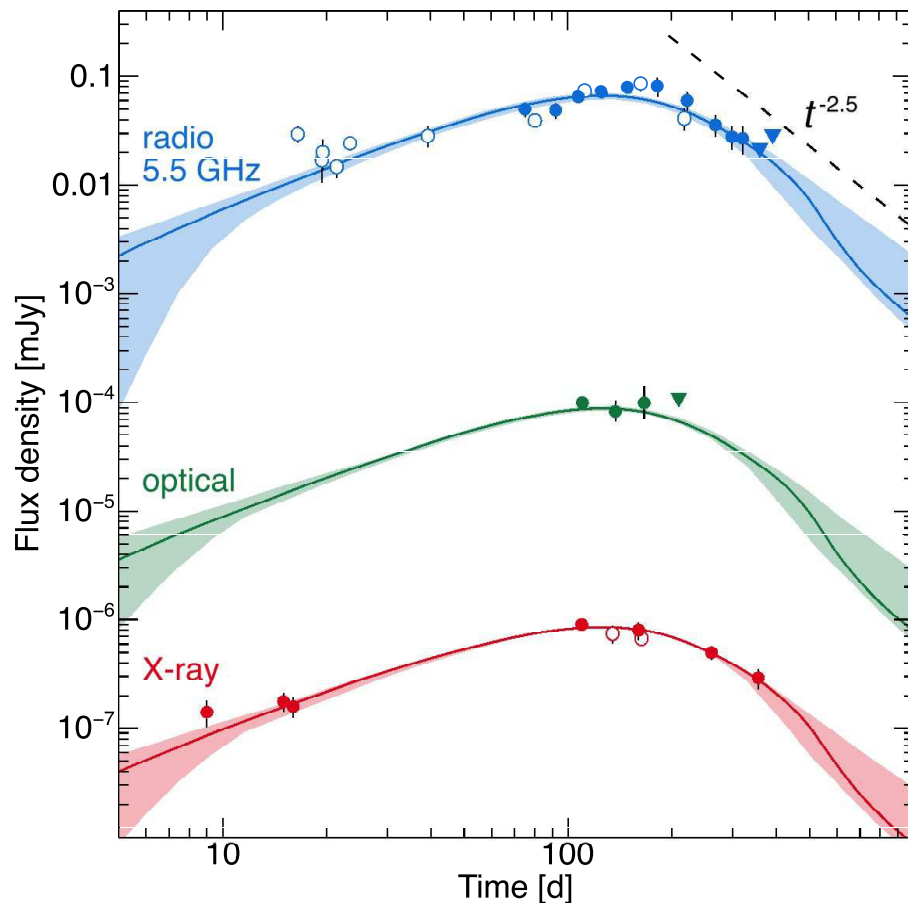

Figure 2. The rise and decay of the afterglow of sGRB 170817A (from [70]).

To date, the afterglow of 170817A can be thus modeled with the standard forward shock scenario, with the only addition of an off-side observer and some structure in the energy density on the jet head. In this scenario, sGRB 170817A may be basically a "normal" short GRB seen off-axis at $\sim 20^0$ from the jet axis. However, among the "anomalies" of this short GRB, there is the fact that the prompt high-energy release assumed isotropy is only $(3.1 \pm 0.7) \times 10^{46}$ erg, four to five orders of magnitude less than usual. Among the proposed hypothesis is that emission from the merger ejecta is heated by the GRB jet when the latter goes out of the ejecta cloud, or "cocoon shock break-out" (see [74] and references therein). However, in this case, the emission should be thermal, but it is not. Alternatively, we may be initially seeing emission from the low-energy "wings" of the jet, which extends up to $\simeq 40^0$ in [70] modeling; apart from this lower energy density of the ejecta, the emission mechanism could be akin to that producing the "normal" prompt emission when the jet is seen on-axis.

Alternative scenarios existed, e.g., a radially stratified spherical outflow ([74] and reference therein). However, polarization studies and the discovery of a super-relativistic point-like radio source demonstrated that a relativistic jet was present ([34,35]). According to the latter studies, the off-axis angle is somehow smaller than that calculated by modeling the sGRB 170817A afterglow, i.e., $\sim 15^0$; however, it is still consistent within the errors.

2.6. Other Short GRBs Hosting Kilonovae

The case of the short GRB 170817A, associated with a gravitational signal and a likely kilonova emission, has spurred the research on such transients in previous short GRBs. Swift/UVOT, as well as ground observatories, might have detected kilonovae events and not recognized them as such [75]. In their work, Ref. [76] (see also [77]) have examined the sGRB of the sample of F15, looking for kilonova signatures in the light curves. First, they took the sample built by F15 and considered mostly (but not exclusively) the events with redshift. After this and other minor cuts and additions, they focused on 39 events. By fitting the UVOT UV and optical data and X-shooter spectra, as well as ground observatory data, they reconstructed 13 AT2017gfo SEDs from UV to NIR and from 0.5 to 10.5 days after the trigger time, and determined the flux density in the filters they were going to use. Subsequently, they compared spectrally and temporally the short GRB afterglow light curves with these templates. They obtained three main sets: GRBs with afterglow weaker than AT2017gfo at least in one filter, short GRBs with shallow decay, and short GRBs with claimed kilonova emission. Moreover, they can separate the blue and the red kilonova components depending on whether they focus on light curves at less or more than 900 nm. Some overlapping is present among the groups. Seven short GRBs fall into the first class (see [76] for details). Their optical counterpart is dimmer than what AT2017gfo would have been at the same epoch and band. The X-ray data could help to disentangle the afterglow vs. kilonova conundrum, but X-ray data are not always available for comparison. Among these, there are sGRB 050709 and sGRB 160821A, for which claims of kilonova emission have been made ([78,79]). For the events of this group, only the kilonova blue component could be constrained, and it has been found that they were 0.2 (at most) - 1 as luminous as AT2017gfo. The exception is sGRB 160821A, for which the red component kilonova was constrained to be 0.4–0.9 as luminous as that of 2017gfo.

For the bursts falling in the second group, we observe a decay too slow to be simple FS emission. The optical band is expected to be between ν_M and ν_C, a regime in which $\alpha = \frac{3}{4}(p-1)$. Since p is generally not predicted to be less than 2, $\alpha \gtrsim 0.75$. Furthermore, AT2017gfo had a slow decay in the blue component only within 1 day after trigger; however theoretical models predict that the KN could peak later. So the target is sGRBs with slow decay before this timescale, but [76] studied also sGRB 050709, whose shallow decay lasted a few days. Several events of this class have a shallow optical light curve; they might be interpreted as energy injection into the KN ejecta by a magnetar, result of the merger. The same magnetar might power the X-ray afterglow, resulting in a shallow decline in both bands. Overall, some of these events would end up with a KN brighter than AT2017gfo,

others with still a weaker one. Eight sGRBs are in the class in which the KN has allegedly been found. Some of them belongs to previous groups as well.

Overall, the blue kilonova range is between ∼17 times brighter and at least ∼5 times weaker (considering upper limits) than that of AT2017gfo; the possible exception being sGRB 070714B, which might have a blue KN more than 200 times brighter than that of AT2017gfo.

The red kilonova range is much more restricted, being between 3 and 0.3 times that in AT2017gfo. However, in the case of sGRB 150424A, for which the redshift is unknown, it is possible that we had a red kilonova 30 times brighter than that of AT2017gfo. But this cannot be confirmed without knowing the redshift.

2.7. GRB 060614: Short GRBs Masqueraded as Long GRBs?

A few GRBs would be classified in the category of "long GRBs" on the basis of duration, but they are actually better interpreted as mergers/sGRB. Chiefly, they do not show any supernova emission, even with deep searches. One example of these events is GRB 060614, an event that Swift/UVOT enabled us to study in great detail. It shows traits of the events classified as "long" GRB, in particular its $T_{90} \simeq 100$ s duration, but no SN was found down to an absolute magnitude $M_V \simeq -14$. We briefly discuss this event since it has an extended UVOT coverage (as well as observations by other telescopes), but we refer the reader to [76,80] and the two following articles for a full, in-depth study.

This burst was in the group of events that has an afterglow flux decay slope too shallow to be simple FS emission, and for which a KN has been claimed ([81,82]; note, however, that [76], with their careful analysis, do not fully support this scenario). The light curves of the afterglow of this event are shown in Figure 3. The GRB 060614 blue filter light curves show a slowly decaying flux up to $\simeq 30$ ks after the trigger time T_0, followed by a phase of decay with slope $\simeq 1$ which lasted from $\simeq 30$ ks to $\simeq 104$ ks. The redder filter light curves, instead, showed a rise up to $\simeq 30$ ks, followed by a phase of decline with slope $\simeq 1$. All optical light curves then break to a steep decline $\alpha \approx 2.44 \pm 0.08$ at $\simeq 104 \pm 22$ ks after the trigger. The X-ray light curve shows an initial slow decay, $\alpha \simeq 0.1$, until epoch $T - T_0 = 36.6 \pm 2.4$ ks, when it breaks to a decay with $\alpha \simeq 1$, and finally at $T - T_0 = 104$ ks becomes a much steeper $\alpha = 2.13 \pm 0.07$. Spectral Energy Distributions (SEDs) were created at 10, 30, 60 and 150 ks. The first SED shows a flat optical spectrum, while the following SEDs show the optical points and the X-ray points lined up. In the frame of the FS model, this event has been interpreted as follows [80]. Around ∼10–20 ks, the synchrotron peak frequency ν_M crosses the optical band in the redwards direction. There is an energy injection [83,84] ending at $\simeq 30$–35 ks, and the decay from 35 ks to $\simeq 104$ ks has the typical FS decay slope of $\alpha \sim 1$. This is visible in the X-ray band as well, whose flux decay becomes steeper with slope $\alpha \simeq 1$ at $T_0+ \simeq 35$ ks. A slope steepening at all wavelengths is expected in the energy injection scenario when such injection ends: indeed, the break time in the X-ray and that in the optical bands is consistent within 3σ.
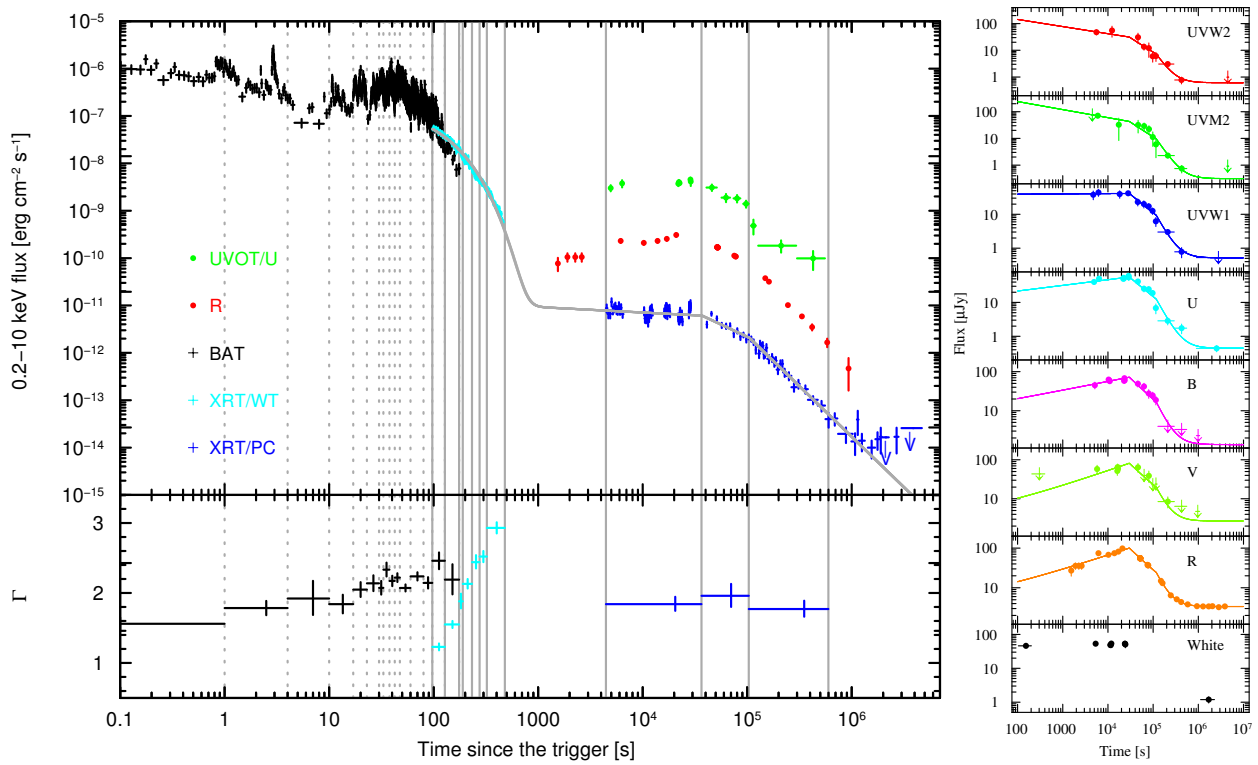
Figure 3. Left: light curves of GRB 060614 in different bands, including X-ray. Right: Individual UV and optical light curves centred on the $\simeq$30 ks break. From [80].

Thereafter, at $\simeq$104 ks, the flux breaks down to a rather steep decay: $\alpha_{3,\text{opt}} \simeq 2.44 \pm 0.08$ in the UVOIR and $\alpha_{3,X} = 2.13 \pm 0.07$: the two decay slopes are consistent within 3σ. This achromatic change of decay index (occurring in both the X-ray, UV and optical bands simultaneously) can be attributed to a jet break. It remains somehow puzzling that the energy injection ended and the transit of ν_M occurred almost at the same time to create the observed light curves; thus, a kilonova occurring at an early epoch should not be discarded. If the emission at $\sim$30 ks is not forward shock emission but kilonova emission, it is $\simeq$17 times brighter than AT2017gfo. If the KN was not present a few hours after the trigger, it might have unfolded later on.

Refs. [81,82] added late HST and VLT data to the UVOT data of GRB 060614. By assuming that the afterglow flux, jet break time, decay slope and spectral slope are those given mostly by UVOT, they could subtract the afterglow component and unveil a substantial second component. According to [81,82], this emission is a KN. However, while [81] argued this using a single data point, Ref. [82] used a few of them. Ref. [82] could fit the few points they derived, and found a good fit for the thermal model. Moreover, the latter authors assume that the emission between 1.7 and 3 days after the trigger is a simple FS power-law synchrotron, with no KN contribution, and extrapolate it to later epochs when the excess should be visible, whereas the former include these epochs in their modeling. According to [82], the second component starts to become evident between $\simeq$3 and $\simeq$4 days and peaks around the latter epoch. However, it is still present up to two weeks after the trigger. At a time $T - T_0 \approx 13.6$ d, Ref. [82] estimate a temperature of 2700 K, while the absolute magnitude is in the range $M_R \simeq -13.5$ (Vega). To obtain such an absolute magnitude, one needs an ejecta mass $\simeq$0.03–0.1 $M_\odot$ and ejecta speeds $\simeq$ 0.2 c. However, these figures could be diminished if one assumes that the rate of deposition of energy into the ejecta is underestimated.

It is important to point out that [76] does not detect such a second component in the late afterglow of GRB 060614. Furthermore, the spectroscopic confirmation of a KN has

occurred only for sGRB 170817A and the recent GRB 230307A. Other cases, including GRB 060614, rely on less decisive photometry.

2.8. sGRB 090510: The Only Short GRB That Triggered Both Swift and Fermi

To date, GRB 090510 [85] represents the only case of a short GRB that triggered both the Large Area Telescope (LAT) [28] instrument onboard Fermi and the BAT instrument onboard Swift. The result is that both satellites observed this event from the very beginning, thus covering a very—and unprecedented at that time—wide spectral range: from Swift/UVOT ($\simeq 0.002$ eV) up to Fermi LAT (20 MeV–300 GeV). The methods used to analyze the LAT data are described in [86]. The light curve of GRB 090510 seen by the LAT instrument shows a possible initial peak at $\simeq 0.3$ s after the GBM trigger T_0, followed by an un-interrupted power-law decay with slope $\alpha_{LAT} = 1.38 \pm 0.07$ and a spectral index of $\beta_{LAT} = 1.1 \pm 0.1$. The last GeV photon is seen at $T - T_0 \simeq 100$ s. The analyzed XRT data were taken from the XRT repository [87,88]. They start at $T_0 + 98$ s and show an initial slow decline with slope $\alpha_{1,X} = 0.74 \pm 0.03$, a break time $t_X = 1.43^{+0.09}_{-0.15}$ ks, and a steeper decay $\alpha_{2,X} = 2.18 \pm 0.10$. The UVOT data were used to produce the optical light curve; after being reduced using standard UVOT ftools, the light curves in the single filters were normalized to the white filter. UVOT observations started $\simeq 100$ s after the trigger. The instrument detected an initial slow rise in the afterglow, with $\alpha_{1,opt} = -0.50^{+0.50}_{-0.13}$, a peak at $t_{peak} = 1.58^{+0.46}_{-0.37}$ ks, and a late decay $\alpha_{2,opt} = 1.13^{+0.11}_{-0.10}$. Adding a constant does not change the fit substantially. Light curves are shown in Figure 4.
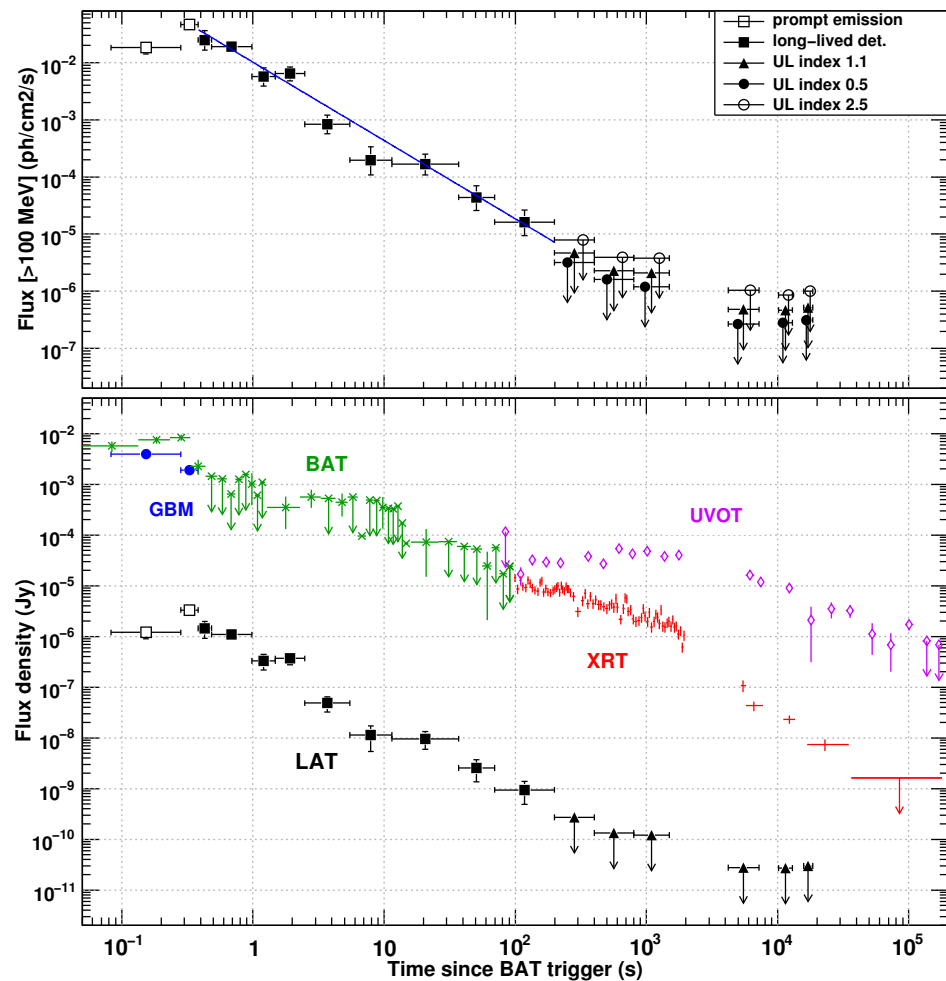

Figure 4. Light curves of GRB 090510 in different bands, as recorded by different instruments. From [85].

VLT observations of the likely host galaxy led to a redshift $z = 0.903$ and an isotropic energy emitted in γ-rays is $E_{\gamma,iso} = 1.08 \times 10^{53}$ erg, making sGRB090510 one the brightest sGRBs detected.

One model to interpret the data can be as follows. The optical is the deceleration peak of the FS emission in a thin medium (in the average denser medium of long GRBs, such a peak occurs a few $\times 100$ s after the trigger; see [89]) while the X-ray and LAT are still late prompt emission. Imposing an initial Lorentz factor of ejecta $\simeq 1000$ (from transparency to photons of GeV energy), a minimum deceleration time of 730 s (from fitting), a peak flux of $\simeq 100$ µJy and $\nu_M \simeq \nu_{opt}$, and a standard $\epsilon_B \simeq 0.01$, from FS equations one obtains that the isotropic kinetic energy $E \gtrsim 5.4 \times 10^{53}$ erg and density $n \lesssim 5.9 \times 10^{-5} \times (E/10^{53})^{-2}$ cm^{-3} [44,90,91].

The XRT and LAT fluxes can be explained by internal shock (IS) synchrotron emission with $\nu_C < \nu_{Opt} < \nu_{SA} < \nu_X < \nu_M$, where ν_{SA} is the synchrotron self-absorption frequency. The synchrotron luminosity, estimated from the 100 s spectral energy distribution, is $L \simeq 10^{50}$ erg/s. One finds [92] that for this value of L and for $p = 2.4$, $\epsilon_e = 0.55$, $\epsilon_B = 0.33$, $\Gamma = 410$, $t_v = 3 \times 10^{-5}$ s, where p, ϵ_e, Γ and t_v are the index of the power-law electron energy distribution, the fraction of energy given to electrons, the bulk Lorentz factor, and the variability timescale, respectively, we have $\nu_M \simeq 210$ keV, F(1.7 keV) $\simeq 75$ µJy, which is within a factor ~ 3 from the observations, and F(100 MeV) $\simeq 4.2 \times 10^{-3}$ µJy, which is consistent within 2σ of the data. The cut-off energy for pair production is h$\nu_{\gamma\gamma} \simeq 1.6$ GeV, thus allowing the late emission of $\simeq 1$ GeV photons. IS does not produce detectable emission in the optical, since this is below $\nu_{SA} \simeq 0.32$ keV.

Another model to explain the observations is as follows. The entire EM emission, from the optical to the LAT band, is forward shock radiation. According to the model, the afterglow broad spectrum consists of three segments: a low-energy tail, with $\beta_1 = -1/3$; an intermediate segment $\nu_M < \nu_{obs} < \nu_C$ with slope $\beta_2 = (p-1)/2$; and a third, high-energy segment with slope $\beta_3 = p/2 = \beta_2 + 1/2$. Five SEDs (see Figure 5) were created from 100 to 12,000 s after the trigger, including UVOT, XRT, LAT data, and fitted simultaneously with the aforementioned FS spectral model template; breaks were allowed to vary. The fit is statistically acceptable, with $\chi^2/\text{d.o.f} = 110.3/83$; the independent spectral index $\beta_{2,X} = 0.77 \pm 0.04$. Thus, in the case of sGRB 090510, the FS model can explain the whole spectrum of the radiation from eV to GeV. In this interpretation, the rise in the optical band is due to peak ν_M approaching the optical band, while the X-ray flux is already decreasing since it lies above ν_M. The late steep X-ray decay is due to a jet break occurring at $t_{jet} \simeq 1.4$ ks. We set the conditions $F_\nu \simeq 2.2$ µJy at 10^{18} Hz, and $\nu_M = 10^{16}$ Hz at 1 ks after the trigger. Using the expression for such quantities from [44], one finds fiducial values for energy and density $\frac{E}{10^{53}} \frac{\epsilon_e}{0.1} \simeq 5$, $n \simeq 1.5 \times 10^{-6} \left(\frac{E}{10^{53}}\right)^{-1} \left[\frac{3(p-2)}{(p-1)}\right]^4$ cm^{-3}. With these values (see [85] for a more complete treatment) the fluxes in the several bands are explained.

One notes, however, that the initial Lorentz factor is rather high, $\Gamma_0 \gtrsim 5800 \left(\frac{E}{10^{53}} / \frac{n}{10^{-4}}\right)^{1/8}$, if the onset of the LAT emission is one second or less. While the spectrum and the fluxes are well explained by this second scenario, the temporal properties are not. First, the initial shallow decay in the X-ray band does not have the slope predicted by the FS [44]. Moreover, even assuming a contribution from the host galaxy, the late optical decay is not consistent with the late X-ray decay (see, however, [93]) as it should be in a jet break regime, and thirdly, the slope of the UVOT spectrum is already red at $T_0 + 1000$ s (see Figure 5) if taken at face value, i.e., the lower frequencies carry more flux density. In our second model, the synchrotron ν_M is still above the optical band at that epoch; as a consequence, the spectrum should be "blue", with more energy carried by higher frequencies. However, the predictions of the FS model are highly idealized and not all GRB afterglows obey them well. In fact, a phase of energy injection (see [83,84]) and/or evolving microphysical parameters of the shock wave might make the early X-ray flux shallow; the transit of ν_M in the optical band slightly after the jet break could explain a shallow decay given the curvature of the spectrum. Some fine-tuning would be needed, however (e.g., jet break nearly at the same time as the rather late transit of ν_M across the optical band). In addition, a jet as early as $\simeq 1.4$ ks implies an opening angle of $\theta_{jet} \simeq 0.004$ rad, i.e., less than a quarter

of degree. Such a narrow jet is not usually observed in GRBs (see [59]), which generally have jets at least an order of magnitude wider.
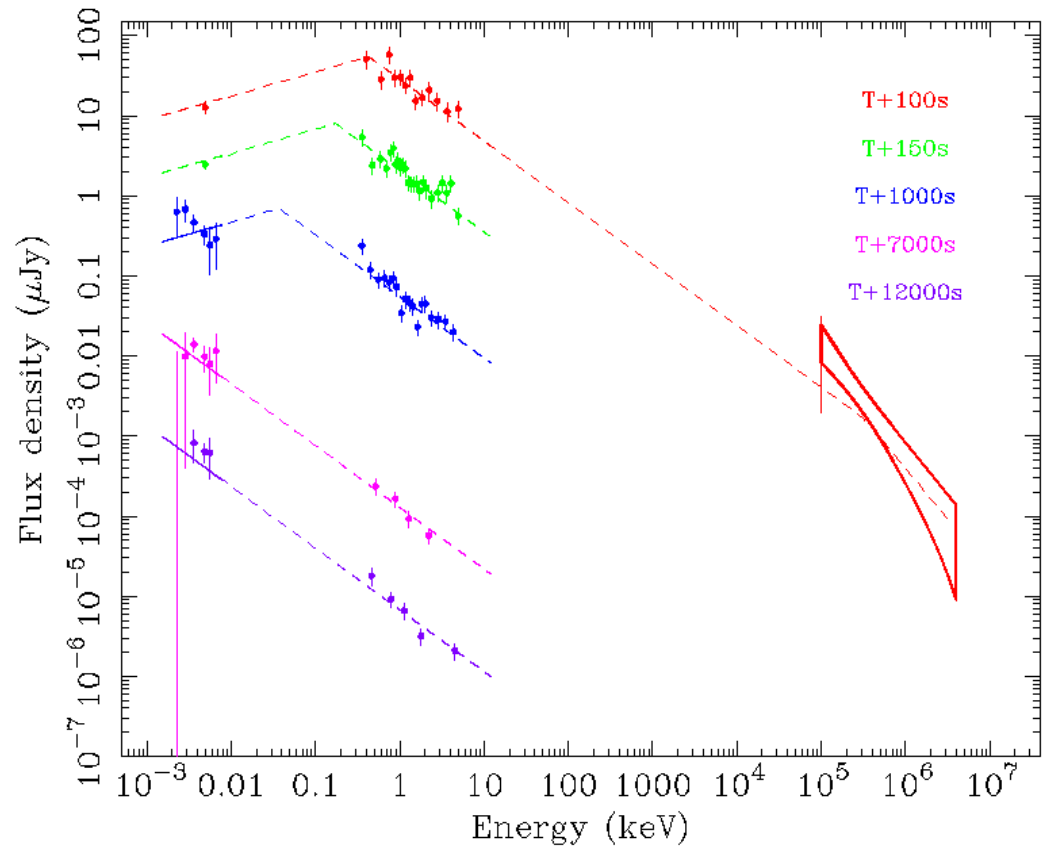

Figure 5. The five SEDs of sGRB 090510 containing data from GeV to eV, fitted simultaneously by a FS spectral template. Successive SEDs in time order are rescaled by 1:1, 1:10, 1:100, 1:1000, 1:10,000. From [85].

3. Discussion

3.1. General Properties of Short GRB in the Swift Era

When F15 systematically examined all sGRBs observed by Swift from the launch to 2015, i.e., more than one hundred events, after removing those with observational constraints, they found that X-ray and optical afterglows are not a rare occurrence in sGRBs; thus, analysis involving the study of the afterglows can be systematically used. By applying broad-band (X-ray, optical including Swift/UVOT, and radio when available) FS-based modeling to the 38 events with best data and with reasonable assumptions of the parameters ϵ_B and ϵ_e, F15 found that the median of circumburst density is of the order of a few $\times 10^{-3}$ cm^{-3}, while the isotropical kinetic energy is of the order of 10^{51} erg, similar to the value of isotropical energy emitted in γ-rays during the prompt. The values above do not change much if ϵ_B or the minimum of the density interval are allowed to be set lower and higher, respectively. The low density obtained is not surprising: sGRBs are often—not always—seen far from their host galaxy and their environment density is not expected to be high. This is in agreement with the idea that sGRB progenitors are a binary NS or BH–NS. Two supernova explosions had to happen to create them, and SNes "kick" the compact objects they produce at hundreds of km s^{-1}. Orbital decay can take billions of years, so by the time the merger occurs, the pairs have traveled far from their birthplace. More unexpected is the fact that a few short GRBs present substantial amount of extinction. On the other hand, some sGRB are found basically within or nearby the disk of their host ([25]), and sGRBs modeled with large densities may be found only in those environments

(but see N22). This finding suggests observing sGRBs with optical filters of UVOT, which are less sensitive to extinction (but see Section 3.4).

Under the assumption that the max semi-opening angle of jetted ejecta $\theta_{jet} < 30$ degrees, F15 found a median $<\theta_{jet}> = 16 \pm 10$ degrees. Remarkably, this is similar to the median beaming angle inferred for long GRBs using the same method: $\theta_{jet,long} = 13^{+5}_{-9}$ degrees.

The true beaming-corrected energy is lower than the isotropic value by a beaming factor $f_b = 1 - \cos\theta_{jet} = 0.04^{+0.07}_{-0.03}$. The sGRB beaming-corrected energy is thus ~ 1.5 orders of magnitude less than the isotropic value; one finds $E_{k,short,beam} \sim E_{\gamma,short,beam} \sim 10^{50}$ erg. These values are important in order to constrain the mechanism able to produce the sGRB. At present, there is more than one mechanisms we think capable to produce an energy of a few 10^{50} erg. For example, $\nu - \bar{\nu}$ annihilation [94], extraction of kinetic energy of the BH remnant of the merger via the Blandford–Znajek mechanism [95], or by a superburst from a massive magnetar outcome of the merger [60]. The similitude between kinetic energy and emitted γ-ray energy tells us of an efficiency in converting the initial total energy into E_γ of $\simeq 50\%$. This efficiency is similar to what is found for long GRBs, perhaps indicating that, once a relativistic jet is launched, the proportion of its energy converted into γ-rays is more or less the same, regardless of the progenitors. However, an efficiency of 50% is not low, and many models for the prompt emission struggle to reach it. Still, some works indicate that this might be possible (e.g., [96]).

The true rate R_{true} of sGRB will be $f_b^{-1} R_{observed}$ the observed one. In fact, the jet break theory implies that, for each short GRB whose high energy prompt emission we detect, there are f_b^{-1} that we do not detect.

Ref. [97] had pointed out that no short GRBs like those occurring at cosmological distances (say, $z \gtrsim 0.2$–0.4) have been detected within the range of gravitational wave detectors (200 Mpc at design; $z \simeq 0.07$) since major orbital, high-energy sensitive facilities are in place. Had this not been the case, we would have seen fantastically bright short GRBs. However, this has never happened. Note that in the sensitive volume of GW detectors (i.e., a sphere of radius $\simeq 0.2$ Gpc), we expect that mergers have taken place since the space era began. Ref. [98] place a "best bet" of ~ 40 y^{-1} NS-NS mergers in the volume in which ALIGO and ALIGO-like detectors will be able to monitor, that is, $\frac{4}{3}\pi\, 0.2^3 = 0.032$ Gpc^3. The current estimate sGRB rate is believed to be ≈ 10 Gpc^{-3} yr^{-1} [99]. Thus, in the volume scanned by GW sensors, we would expect ~ 0.3 events y^{-1}; facilities that have observed the whole sky over many years now have not seen this rate of very bright sGRB, and the short GRBs without redshift are rather weak events [97]. An even higher estimate of the sGRB rate was obtained by [100]. By using a Lynden–Bell c-method to determine the luminosity function of sGRBs and their rate, they find that the latter is $203.31^{+1152.09}_{-135.54}$ Gpc^{-3} yr^{-1}. If every short GRB produced a GW signal, we would have ~ 0.8 signal yr^{-1} (for the horizon of $\simeq 100$ Mpc in the O4 run; at detector design sensitivity, the rate should rise to $\simeq 6$ signals yr^{-1}).

To reconcile the dearth of nearby sGRBs with the best-bet number of mergers, one thus needs a local population of on-axis weak sGRBs, a semi-opening angle narrower than 16^0 (so a larger fraction of sGRBs beam their jets away from us), not all mergers to bring about a short GRB because the right conditions are not met, and/or the true rate of mergers in the local Universe to be less than that predicted. For example, if the semi-opening angles of the jet were $\theta_{jet} \simeq 7^0$, then $f_b \simeq 0.007$ and only 1 merger in every 130 will have its prompt emission pointing towards the Earth. This is within the errors for the beaming factor found by F15. In this scenario, there will be "normal" sGRBs occurring within 200 Mpc, but if the observer is off-axis, because of relativistic effects, the derived γ-ray fluence will be much smaller than in the usual, bright on-axis sGRBs. So, we may well miss the prompt Gamma-ray emission completely. Instead, we might detect the delayed afterglow emission if the observer is not too off-axis [72]. In the Methods, we have indicated how an off-axis sGRB might explain the rise and decay in the afterglow emission with a peak $\simeq 5$ months after the trigger, as seen in sGRB 170817A (see Figure 2).

All of that is important for GW detectors. In fact, GW radiation is emitted by the merger roughly isotropically. Thus, it might well be detected in coincidence with a weak sGRB, or without an sGRB at all. Furthermore, kilonova emission is approximately isotropic as well; thus, it can be detected if the sGRB is absent or too far off axis [101], and the afterglow may also be detected if an sGRB has followed the merger and the observer is not too far off axis.

This was confirmed with GW 170817A/sGRB 170817A/AT2017gfo. A GW signal, flagging the merger of two neutron stars, was first detected. Almost simultaneously, a very weak short GRB was detected in the error region by the Fermi GBM. A few hours later, a new optical source, having properties unmatched by anything known, was found as well in the error region. This optical source did not have the properties of a GRB afterglow, but it was due to the glowing ejecta of the merger: the so-called kilonova. Finally, the afterglow emission showed up with its characteristic power-law spectrum.

As mentioned in Methods, Refs. [34,35] have proven that a relativistic jet was produced in the case of sGRB 170817A. Such an analysis led to an off-axis angle $\simeq 15$ degrees from the Earth's observer. Modeling of the afterglow, as we have seen, leads to a slightly larger off-axis angle. Anyway, both kinds of study give results that are consistent within errors, and importantly they abide by the GW data analysis result put forward, according to which we were observing the binary with an an off-axis angle less than $\simeq 30^0$ [102]. In such conditions, we would have first seen the kilonova and later on a rising afterglow in all bands (not immediately after the prompt, as in "on axis" GRBs). This seems to be what happened.

Theoretical work and observations are instead needed to explain the weak high energy prompt emission of sGRB 170817A, which is 4–5 order of magnitudes less than that of usual short GRBs. Most models put the observer at considerable distance from the core of the ultrarelativistic jet, implying that it can hardly contribute to prompt emission. In fact, the fluence one would see off-axis goes as $\simeq [(\theta_{obs} - \theta_{core}) \cdot \Gamma]^{-6}$ [72]. Thus, for a fiducial $\theta_{core} \simeq 4.5$ degrees, an observing angle $\theta_{obs} \simeq 20$ degrees [70], and an initial Lorentz factor $\Gamma \simeq 100$, one has a reduction in the fluence, and thus a diminution of the inferred energy by a factor of $\sim 10^8$. One must thus invoke alternative models. In a structured jet (see [74] and reference therein), there are less energetic wings surrounding the core. For example, in the modeling of [70], the observer is off-axis but the line of view is still within the opening angle of jet wings. Thus, the mechanism creating the prompt emission of GRB 170817A might still be the unclear mechanism that typically produces the prompt emission in GRBs, but the ejecta that produce it are wing ejecta, and are quite off-axis. They have less energy per unit surface than the core ejecta that create the typical GRBs. Thus, this mechanism yields a weaker prompt emission. For example, assuming a Gaussian distribution of energy throughout the surface of the jet, for $\theta_{core} = 4.5$ degrees and $\theta_{obs} = 20$ degrees (values fully consistent with the modeling of [70] and the GW radiation received), the energy per unit surface is only $\sim 5 \times 10^{-5}$ that it would be measured if the observer saw the core of the jet. Alternatively, the jet may heat the ejecta along the polar axis, causing the production of a cocoon which will "break out" when the jet reaches the surface of the cocoon. A flash of hard and much less beamed radiation is then expected. However, such a radiation should still be thermal, but the spectrum of the prompt emission of sGRB170817A is not thermal.

3.2. Host Galaxies of Short GRBs

While some contamination from false sGRB–host galaxy associations are practically guaranteed, F22 were right in including less-certain host–sGRB associations in their sample, since one would like to study also sGRBs whose progenitors have suffered strong natal kicks and moved far away from their birth place and bursts which have faint host galaxies. In addition, including photometric redshifts avoided the so-called "redshift desert" at $z \gtrsim 1$, where the prevalent spectral features to identify the redshifts are lacking. In this respect, knowing the redshift distribution of sGRBs is a powerful instrument to constrain the distribution of delay times and, in turn, rule out or accept ways for the formation of progenitor systems. F22 found that $\sim 1/3$ of sGRBs likely originate at $z \gtrsim 1$. The deep observations of F22 practically guarantees that all hosts at $z \lesssim 1$ and brighter than 10^9 L$_\odot$

have been detected; however, this value is, for example, still higher than the typical low-luminosity hosts of long GRBs. This suggests that one requires a sizeable amount of stellar mass to have an sGRB (see below). Intriguingly, F22 found that, even taking into in account the larger sizes of sGRB host galaxies, sGRBs explode at a distance that, normalized to the light radius of the host, is still on average $\simeq$2.5 times larger that of long GRBs. The presence of sGRBs with no clearly related host (F22) could simply be due to the very long path taken by the progenitor system: they might have moved so far from their birth place that we cannot associate them anymore to a certain galaxy. Moreover, the presence of such distances between the hosts and the merging binary indicates that the process that moves the progenitor away from the host can be quite efficient.

Short GRB progenitors can form in many environments over a large range of redshifts and star formation histories (N22). However, there is still a relative deficit of massive hosts when compared with field galaxies. Since sGRB hosts still follow the SFMS, one can argue that these bursts follow a combination of star formations and stellar masses together. Another very important finding of N22 is obtaining a strong indication for *two populations of progenitors*: a short-delay-time one, which is present in young and actively star-forming galaxies, and is the large majority of observed events at $z \gtrsim 0.25$, and a long-delay-time one, which prevails at $z \lesssim 0.25$ and it is associated with quiescent galaxies. In this respect, it is interesting to note that the typical distance between the host and the sGRB is larger if the host is quiescent: the median offset is $\approx$9 kpc if the host is star-forming, while it rises up to $\approx$26 kpc if the host is quiescent. This difference almost disappears if one divides by the light radius. Nonetheless, it does take longer to reach the latter distances (if the speed is similar); thus, it is not unreasonable to assume that progenitors originating from quiescent galaxies were born when these galaxies were somehow forming stars as well. Through modeling with PROSPECTOR ([54]), N22 significantly increased the known limits of redshifts and shed light on the stellar population properties probed by short GRBs. Furthermore, their study of host properties can constrain specific NS binary quantities, such as natal kicks, orbital distances, and delay times. Moreover, since NS mergers are known to produce some (if not most) of the r-process elements in the Universe, a better comprehension of their redshift distribution would enable us to grasp when in the Universe's history these elements were generated and how much mergers contributed. Usefully, given that sGRBs seem to trace stellar mass *and* star formation in galaxies, the future hunt for EM counterparts could be arranged to account for that, rather than simply following up massive but passive galaxies. sGRBs are presently found much more frequently at redshifts larger than those of GW-detected NS-NS mergers. Thus, while room for improvement exists—for example determining the spectroscopic redshift rather than the photometric for the sGRBs and events at $z > 1$ with the JWST— N22's work provides a heritage that will not be matched by GW detections for at least several years to come.

3.3. Kilonovae: AT2017gfo and Other Sources

As mentioned above, the kilonova is thought to derive from the self-heating ejecta of the merger ejecta. Still, the Swift/UVOT detection of a substantial yet short-lived UV and blue thermal component in the kilonova emission during the first day after the trigger was surprising and had important implications; many models of KNe do not reproduce this feature. Kilonovae were thought to be basically very opaque, and thus able to emit only in the red and infrared part of the spectrum [103]. This was believed to be especially true if the emitting material was dynamical ejecta—those produced by tidal stripping or at the moment of impact of the two bodies. These ejecta would be very rich in neutrons (electron fraction $Y_e \lesssim 0.2$), and should produce large quantities of r-elements having high mass numbers such as $\sim$82, $\sim$130 and $\sim$196 (the so-called first, second and third peak r-elements; [104]). Some of the nuclei will have too many neutrons, which decay into protons and create new elements, in addition to heating the ejecta. The complex and numerous atomic transitions in the atoms and ions of the lanthanides and of the actinides elements would be responsible for the large opacity of such ejecta. Clearly, not all the

ejecta in AT2017gfo were of this kind, or we would have never seen the UV emission. The general consensus is that the early emission was produced by *wind* ejecta, which are created *after* the merger in magnetic and/or viscous processes and/or are neutrino-driven outflows from the possible Hyper-Massive Neutron Star, the outcome of the merger, and/or its accretion disk. The HMNS may support itself thanks to its fast rotation, but then it loses enough energy and angular momentum via GWs and/or neutrino winds and collapses into a black hole. The wind ejecta are less neutron-rich than the dynamical ejecta, especially if they are exposed to neutrino winds of the HMNS and/or the disk, with values of $Y_e \simeq 0.2$–0.4 regarded as possible. The outcome of such a large electron fraction is that r-nucleosynthesis is stopped at the second or even the first r-process peak; this results in no actinides and little lantanides, if any, being made. As a consequence, the wind ejecta are more transparent and are responsible, together with the early high temperature of the ejecta, for the blue kilonova phase. Later on, the emission from the opaque and faster dynamical ejecta takes over. As mentioned above, [31] find a good fit to the data for $Y_{e,\,wind} \lesssim 0.27$, velocity $v_{wind} = 0.08$ c and $Y_{e,\,dyn} \simeq 0.04$, $v_{dyn} \simeq 0.3$ c (Figure 6; considering black-body emission). The mass of the wind ejecta must be substantial, at least of the order of 0.03 $M_\odot$ to reproduce the results. We emphasize that, without Swift/UVOT UV and *u* observations, we would today know less of the important "blue" phase of kilonovae and the presence of lighter elements. Having established that a sizeable production of the r-elements can broadly explain the properties of KNe observed in mergers, one may wonder if they can be responsible for the abundance of r-elements detected, for example, in the Milky Way. According to [64] (see also references therein), for the expected rate of $\sim$1000 mergers Gpc^{-3} yr^{-1}, one can roughly explain the quantity of such elements. Production in core-collapse SNe is still possible, but mergers would still be the dominant source of r-elements.
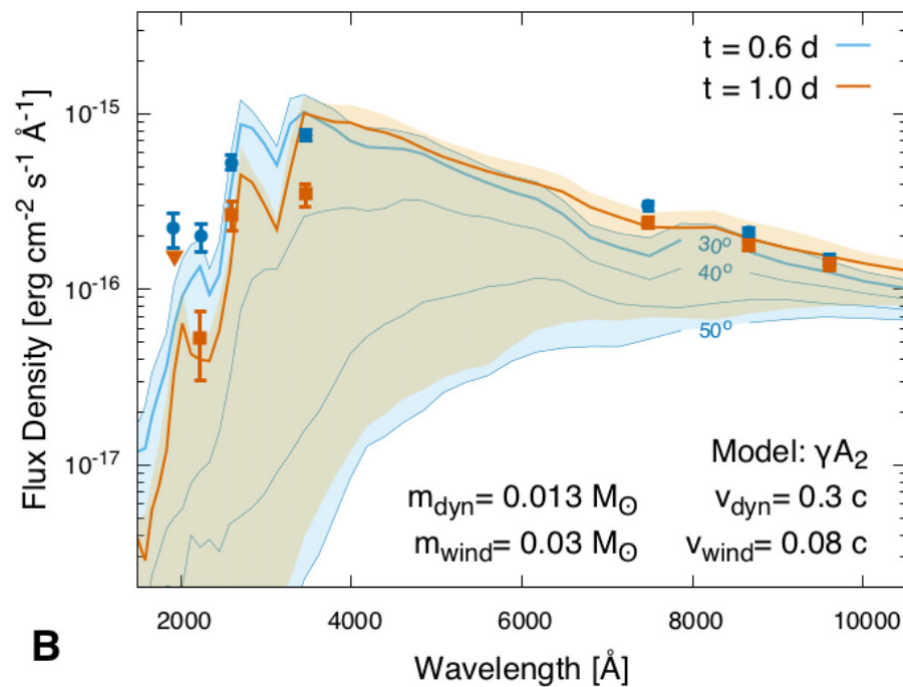

Figure 6. Two-component kilonova model: "blue" (low opacity) and "red" (high opacity) components that best fit data ([31]).

The energy lost by the jet during the burrowing would go to an cocoon made of ejecta material that has been invoked to produce the prompt—and thermal—emission. However, the high energy prompt emission of sGRB 170817A does not show a thermal spectrum. Models such as the hot cocoon for the prompt emission are disfavored in this case; however, in other mergers, it is possible that the jet did not make through the ejecta and the high

energy emission would be produced by the heated ejecta. This thermal emission may be detected by instruments such as XRT and UVOT if observations are started early enough. On this theme, the discovery of a kilonova spurred attention on other nearby sGRBs that may have it combined with the afterglow emission. However, these sGRBs were seen on-axis; thus, the prompt emission and the initial afterglow would have been much brighter than in the case of 170817A. Kilonovae have been claimed to be detected in a few short GRBs (see [75–78] and references therein); analyses of the light curves seem to indicate that the luminosity of the blue component of KNe, like that seen early in AT2017gfo, may vary between ≲0.2 and ∼17 (and perhaps 260) in that event. The most extreme cases may be energized by a magnetar, a stable (at least for an appreciable amount of time) outcome of the NS-NS merger [105]. Present studies seem to indicate that there is a lot of latitude in the mass and energy coupled with the wind ejecta, but little variability in the dynamical (disk) ejecta.

3.4. The "Progenitor" of GRBs: The Real Distinction between Long and Short GRBs

GW 170817A—sGRB 170817A has definitively linked short GRBs and mergers of neutron stars (at least in a few cases). Generally speaking, the collision of the two NS may not lead immediately to the collapse into a black hole; if this had been the case, we would have likely seen little ejecta and kilonova emission in that sGRB and others. Instead, the merger may result in an object that would sustain itself thanks to its rotation (see [60] and references therein), until losing enough energy and angular momentum through neutrino winds and GWs to collapse into a black hole—the aforementioned HMNS. Meanwhile, it is possible that instabilities make the magnetic field of the disk surrounding the central object grow to gargantuan levels of $\sim10^{17}$ gauss or more, while MHD simulations show that conical funnels open along the polar axis of the central object, with semi-opening angles of ∼20 degrees. If the BH forms in a fraction of second, it is still surrounded by the accretion disk; it couples magnetically with the disk material and powers the jets into the funnels according to the Blandford–Znajek mechanism, which can easily produce the $\sim10^{50}$ erg of a sGRB. The opening angle of the funnels would also be similar to the median angle of short GRB jets (see the section on physical parameters of sGRBs). Note, however, that other mechanisms might produce the jet of such an energy, such as the annihilation of neutrinos-antineutrinos produced by the accretion disk. See [60,74] for more details. If the result of the merger does not collapse into a black hole at all (or it does not for a long time), and has a magnetar-like magnetic field, it can output energy at roughly constant rate [83,106] via dipole radiation, causing flat plateaux in the afterglow optical and X-ray light curves (see also [107]). However, this would be an indirect hint of the presence of a magnetar. It is also supposed that a weak jet or no jet would form if the central object does not collapse into a black hole within ∼1 s, since the disk is expected to dissipate [60].

The hallmark of a merger is the kilonova emission: if it is present, the GRB comes from a merger, whereas if the event is associated with a energetic SN, it is initiated by the collapse of a massive star. The length of the prompt emission is a poor indicator to tell apart GRBs caused by mergers and those brought about by a massive stellar progenitor. Note, in addition, that a merger and kilonova may be present even if the physical conditions have not led to a sGRB. In such a case, we would still detect a GW signal followed by the KN. Remarkably, kilonova emission has been now found in GRBs that we would classify as "long GRBs", recent examples being GRB 211211A [75,108] and 230307A [63]. Such events, however, share some commonalities with short GRBs. Their prompt light curve is typically a hard, short spike, followed by a much softer "prompt" emission. Their lags among the prompt emission bands is not similar to that of long GRBs. Instead, these events might be like GRB 060614 and sGRB 050724—if the KN is present in them—but brighter. Swift/UVOT has again contributed to constraining the properties of the KNe associated with these GRBs thanks to the rapid response and UV sensitivity. It is possible to argue that GRB 211211A and 23037A are actually short GRBs, in the sense that they are produced by

the merger of a binary NS or a NS-BH system, but a particularly bright extended emission make them look like long GRBs.

While detecting the kilonova of an on-axis sGRB seems to be possible, obviously it is much easier—and can produce more precise data—if the merger is seen off-axis. Catching the merger off-axis is also much more likely than on-axis (as mentioned before, there might be ∼40 events y^{-1} in the GW detectors at design sensitivity), and may lead to a "clean" kilonova emission, not contaminated by the prompt and/or afterglow emission. If GRBs are a truly jetted source as 170817A seems to confirm, geometry is in our favour: we shall "see" many more off-axis merger events than on-axis ones, still associated with a GW signal. We remind that even if the merger of two NS does not lead to an sGRB because the conditions are not right, a GW signal is expected and a KN may well occur anyway.

Following what we learnt with GW 170817/AT2017gfo and akin sources, it is perhaps advisable that EM observation of the GW source error region should contain exposures in UV and *u* band, in addition to observations at redder frequencies for the extinguished sources. It is thus clear that the Swift/UVOT will remain an essential tool in the future of "multi-messenger" astrophysics.

3.5. sGRB090510: One of the Brightest Short GRBs, Which Triggered both Swift and Fermi

Swift/UVOT greatly contributed to study the bright sGRB 090510, the only short burst to date so bright that it triggered both Fermi LAT (in the GeV band) and Swift BAT, leading to simultaneous, and at the time unprecedented, observations from the very beginning over nine decades of frequency. The UVOT data were pivotal in the efforts of modeling the afterglow of this event; UVOT coverage started ∼100 s and ended ∼2 × 10^5 s after the trigger. In [85], two scenarios are put forward to explain observations. In the first, one tries to explain the opposite behavior of early X-ray (decreasing) and optical flux (increasing). The X-ray and LAT flux is due to shocks occurring inside the ejecta (internal shocks (IS)), while the whole optical emission is attributed to the standard FS. This scenario requires very low densities (but compatible with the intergalactic medium (IGM)) of the order of few 10^{-6} cm^{-3}. Such low densities are expected because the progenitor might have been expelled from the host galaxy by two successive supernova explosions. The model does not need an extremely large value of Lorentz factor of the ejecta. The required values of the physical parameters involved are reasonable, although some fine tuning is needed.

In the second scenario, all EM emissions from eV to GeV are FS radiation. We find that a simultaneous fit of five SEDs, including LAT, XRT, and UVOT data (a spectrum as wide as nine orders of magnitude in frequency), built at different epochs with the FS spectral template is statistically satisfactory, and most physical parameters needed are reasonable, although the initial Lorentz factor will have to be bigger than 5000 and a jet break should occur at as early as 1400 s. Still, the most basic version of this FS model fails to reproduce the observed temporal behavior; some common extensions of this scenario and some fine tuning is needed to accommodate the results. If this short GRB indeed underwent a very early jet break, then UVOT data, together with XRT data, were essential to constrain the time of its occurrence. UVOT could then help us unveil GRBs with very early jet breaks, which in turn imply very narrow beaming angles and rates larger than thought previously.

3.6. Is the Central Engine Always the Same?

Last but not least, we remark that observations so far presented may suggest diversity in the physical parameters of the sGRB central engine.

The prompt, high-energy radiation, which is thought to be produced directly in the ejecta of the central object, may differ a lot in sGRBs. In some cases, the prompt emission looks like that of a long GRB, and yet a KN component is present in the later optical afterglow, thus indicating that the origin of such bursts lies in mergers.

The "blue" kilonova luminosity may vary a lot among bursts [76], while the "red" kilonova is more or less of the same order of magnitude among different events. This may, in turn, indicate that the amount of slow, wind-like ejecta produced close to the

central object and made of r-elements with low neutron numbers may change a lot among different events, whereas the amount of heavier r-elements that should be produced in the pre-merger tidal ejecta is roughly the same under different conditions.

At least two different channels—one quick, one taking billions of years—seem to bring about mergers, which may thus have different physical parameters for the two modalities, leading to central objects with different properties.

The possibility that the the post-merger central object might have quite different parameters could help explain why, according to population studies, there are much more local mergers than short GRBs, even considering beamed sources. The parameters of some mergers may not always lead to creating an ultra-relativistic jet and a dissipation mechanism in them to have short GRBs.

4. Conclusions

sGRBs have allowed us to enter the "multi-messenger" era of astronomical research: we can detect NS-NS (and NS-BH) mergers by means of both electromagnetic waves and gravitational waves. GWs allow us to gather information on the "inner workings" of some of the most violent phenomena in nature. The EM observations, on the other hand, have confirmed basic theoretical predictions, such as the kilonova and the off-axis afterglow emission. However, when we go into details, there is still a lot to learn.

Modelling and studying of the prompt and afterglow emission of sGRBs, as well as host population studies, have shown diversity in lengths of the prompt emission, "blue kilonova" luminosity due to material emerging from the vicinity of the central object result of the merger, and the time needed for the compact object binary to merge. All these clues may indicate that the central engine of short GRBs can be quite diverse and sometimes the conditions to create the ultrarelativistic jet and/or dissipation mechanism in it are not met.

We have not pinned down the process that produced the weak-prompt Gamma-ray emission in the case of sGRB 170817A, nor do we know the precise structure of the jet as it emerges from the merger wind/ejecta, and we still do not know very well the number of r-elements globally produced by the sGRB and released into the Universe. This can be clarified only by spectroscopically studying more KNe and knowing more precisely the rate of mergers involving NSs which, as we mentioned before, can be different from the rate of sGRBs, even off-axis ones.

The Swift/UVOT will continue to provide us with data of crucial importance, which, at present, cannot be obtained by other instruments. Very powerful supercomputers are needed to study what happens in the extreme conditions occurring when an NS-NS or BH-NS binary merge, and under which conditions a jet and an sGRB can be produced.

From both the observational and the theoretical computational sides, the study of sGRBs seems to promise very important advancements in physics and astronomy in the years to come.

Abbreviations

The following abbreviations are used in this manuscript:

2MASS	Two micron all sky survey
BAT	Burst alert telescope
BH	Black hole
CCD	Charged-coupled device
CGRO	Compton Gamma-ray Observatory
EM	Electromagnetic
F15	Fong et al. (2015)
F22	Fong et al. (2022)
FS	Forward shock
FWHM	Full width at half maximum
Gaia DR	Gaia data release
GBM	Gamma-ray burst monitor
GeV	Giga electron volt
GW	Gravitational wave
GRB	Gamma-ray burst
sGRB	short Gamma-ray burst
HMNS	Hyper-massive neutron star
HST	Hubble Space Telescope
IGM	Intergalactic medium
IRAF	Image reduction and analysis facility
IS	Internal shock
KN	Kilonova
JWST	James Webb Space Telescope
LAT	Large area telescope
N22	Nugent et al. (2022)
NS	Neutron star
Pan-STARRS	Panoramic survey telescope & rapid response system
(Beppo)SAX	Satellite per astronomia X
SDSS	Sloan digital sky survey
SED	Spectral energy distribution
SExtractor	Source-extractor
SFMS	Star-forming main sequence
SFR	Star formation rate
UVOT	UV/Optical Telescope
UVOIR	UV optical infrared
XRT	X-ray telescope
Z	Metallicity
S/N	Signal/Noise ratio

Notes

1. The duration is measured as T_{90}, defined as the time interval to collect 90% of the source counts by the detector

2. https://heasarc.gsfc.nasa.gov/lheasoft/ftools/caldb/help/uvot.html, (accessed on 30 August 2017)

References

1. Klebesadel, R.W.; Strong, I.B.; Olson, R.A. Observations of Gamma-ray Bursts of Cosmic Origin. *Astrophys. J.* **1973**, *182*, L85. [CrossRef]
2. Gehrels, N.; Fichtel, C.E.; Fishman, G.J.; Kurfess, J.D.; Schönfelder, V. The Compton Gamma-ray Observatory. *Sci. Am.* **1993**, *269*, 68. [CrossRef]
3. Kouveliotou, C.; Meegan, C.A.; Fishman, G.J.; Bhat, N.P.; Briggs, M.S.; Koshut, T.M.; Paciesas, W.S.; Pendleton, G.N. Identification of two classes of Gamma-ray Bursts. *Astrophys. J. Lett.* **1993**, *413*, 101. [CrossRef]
4. Bromberg, O.; Nakar, E.; Piran, T. An observational imprint of the collapsar model of long gamma-ray bursts. *Astrophys. J.* **2012**, *749*, 110. [CrossRef]
5. Piro, L. SAX, the wide band mission for X-ray astronomy. *MmSAI* **1996**, *67*, 575. [CrossRef]

6. Costa, E.E.; Frontera, F.; Heise, J.; Feroci, M.A.; In't Zand, J.; Fiore, F.; Cinti, M.N.; Dal Fiume, D.; Nicastro, L.; Orlandini, M.; et al. Discovery of an X-ray afterglow associated with the γ-ray burst of 28 February 1997. *Nature* **1997**, *387*, 783. [CrossRef]

7. De Pasquale, M.; Piro, L.; Gendre, B.; Amati, L.; Antonelli, L.A.; Costa, E.; Feroci, M.; Frontera, F.; Nicastro, L.; Soffitta, P. The BeppoSAX catalog of GRB X-ray afterglow observations. *Astron. Astrophys.* **2006**, *455*, 813. [CrossRef]

8. Fruchter, A.S.; Levan, A.J.; Strolger, L.; Vreeswijk, P.M.; Thorsett, S.E.; Bersier, D.; Burud, I.; Castro Cerón, J.M.; Castro-Tirado, A.J.; Conselice, C.; et al. γ-ray bursts and core-collapse supernovae have different environments. *Nature* **2006**, *441*, 463. [CrossRef]

9. Galama, T.J.; Vreeswijk, P.M.; Van Paradijs, J.; Kouveliotou, C.; Augusteijn, T.; Böhnhardt, H.; Brewer, J.P.; Doublier, V.; Gonzalez, J.F.; Leibundgut, B.; et al. An unusual supernova in the error box of the γ-ray burst of 25 April 1998. *Nature* **1998**, *395*, 670. [CrossRef]

10. Hjorth, J.; Bloom, J.S. The GRB-SN Connection. In *Gamma-ray Bursts*; Kouveliotou, C., Wijers, R.A.M., Woosley, S., Eds.; Cambridge University Press: Cambridge, UK, 2012; pp. 169–190.

11. Bloom, J.S.; Kulkarni, S.R.; Djorgovski, S.G. The Observed Offset Distribution of Gamma-ray Bursts from Their Host Galaxies: A Robust Clue to the Nature of the Progenitors. *Astron. J.* **2002**, *123*, 111. [CrossRef]

12. Eichler, D.; Livio, M.; Piran, T.; Schramm, D.N. Nucleosynthesis, neutrino bursts and γ-rays from coalescing neutron stars. *Nature* **1989**, *340*, 126. [CrossRef]

13. Narayan, R.; Paczyński, B.; Piran, T. Gamma-ray Bursts as the Death Throes of Massive Binary Stars. *Astrophys. J.* **1992**, *395*, L83. [CrossRef]

14. Gehrels, N.; Chincarini, G.; Giommi, P.E.; Mason, K.O.; Nousek, J.A.; Wells, A.A.; White, N.E.; Barthelmy, S.D.; Burrows, D.N.; Cominsky, L.R. et al. The Swift Gamma-ray Burst Mission. *Astrophys. J.* **2004**, *611*, 1005. [CrossRef]

15. Barthelmy, S.D.; Barbier, L.M.; Cummings, J.R.; Fenimore, E.E.; Gehrels, N.; Hullinger, D.; Krimm, H.A.; Markwardt, C.B.; Palmer, D.M.; Parsons, A.; et al. The Burst Alert Telescope (BAT) on the SWIFT Midex Mission. *Space Sci. Rev.* **2005**, *120*, 143. [CrossRef]

16. Burrows, D.N.; Hill, J.E.; Nousek, J.; Kennea, J.A.; Wells, A.; Osborne, J.P.; Abbey, A.F.; Beardmore, A.; Mukerjee, K.; Short, A.D.T. et al. G The Swift X-ray Telescope. (XRT). *Space Sci. Rev.* **2005**, *120*, 165. [CrossRef]

17. Roming, P.W.; Kennedy, T.E.; Mason, K.O.; Nousek, J.A.; Ahr, L.; Bingham, R.E.; Broos, P.S.; Carter, M.J.; Hancock, B.K.; Huckle, H.E.; et al. The Swift Ultra-Violet/Optical Telescope. *Space Sci. Rev.* **2005**, *120*, 95. [CrossRef]

18. Still, M.; Roming, P.W.A.; Mason, K.O.; Blustin, A.; Boyd, P.; Breeveld, A.; Brown, P.; De Pasquale, M.; Gronwall, C.; Holland, S.T.; et al. Swift UVOT Detection of GRB 050318. *Astrophys. J.* **2005**, *635*, 1187. [CrossRef]

19. Schady, P.; Pagani, C. Swift/UVOT Observations of GRB 060313. *GCN* **2005**, 4877.

20. Kann, D.A.; Klose, S.; Zhang, B.; Covino, S.; Butler, N.R.; Malesani, D.; Nakar, E.; Wilson, A.C.; Antonelli, L.A.; Chincarini, G.; et al. The Afterglows of Swift-era Gamma-ray Bursts. II. Type I GRB versus Type II GRB Optical Afterglows. *Astrophys. J.* **2011**, *734*, 96. [CrossRef]

21. Sari, R.; Piran, T; Narayan, R. Spectra and Light Curves of Gamma-ray Burst Afterglows. *Astrophys. J. Lett.* **1998**, *497*, 17. [CrossRef]

22. Gehrels, N.; Sarazin, C.L.; O'brien, P.T.; Zhang, B.; Barbier, L.; Barthelmy, S.D.; Blustin, A.; Burrows, D.N.; Cannizzo, J.; Cummings, J.R.; et al. A short γ-ray burst apparently associated with an elliptical galaxy at redshift z = 0.225. *Nature* **2005**, *7060*, 851. [CrossRef] [PubMed]

23. Berger, E. Short-Duration Gamma-ray Bursts. *Annu. Rev. Astron. Astrophys.* **2014**, *52*, 43. [CrossRef]

24. Fong, W.F.; Berger, E.; Margutti, R.; Zauderer, B.A. A Decade of Short-duration Gamma-ray Burst Broadband Afterglows: Energetics, Circumburst Densities, and Jet Opening Angles. *Astrophys. J.* **2015**, *815*, 102. [CrossRef]

25. Fong, W.; Nugent, A.E.; Dong, Y.; Berger, E.; Paterson, K.; Chornock, R.; Levan, A.; Blanchard, P.; Alexander, K.D.; Andrews, J.; et al. Short GRB Host Galaxies. I. Photometric and Spectroscopic Catalogs, Host Associations, and Galactocentric Offsets. *Astrophys. J.* **2022**, *940*, 56. [CrossRef]

26. Hjorth, J.; Sollerman, J.; Gorosabel, J.; Granot, J.; Klose, S.; Kouveliotou, C.; Melinder, J.; Ramirez-Ruiz, E.; Starling, R.; Thomsen, B.; et al. GRB 050509B: Constraints on Short Gamma-ray Burst Models. *Astrophys. J. Lett.* **2005**, *630*, 117. [CrossRef]

27. Fritschel, P. et al. [LIGO Scientific Collaboration]. Advanced LIGO. *arXiv* **2014**, arXiv:1411.4547.

28. Meegan, C.; Lichti, G.; Bhat, P.N.; Bissaldi, E.; Briggs, M.S.; Connaughton, V.; Diehl, R.; Fishman, G.; Greiner, J.; Hoover, A.S.; et al. The Fermi Gamma-ray Burst Monitor. *Astrophys. J. Lett.* **2003**, *585*, 885.

29. Abbott, B.P. et al. [LIGO Scientific Collaboration and Virgo Collaboration, Fermi Gamma-ray Burst Monitor, and INTEGRAL] Gravitational Waves and Gamma-rays from a Binary Neutron Star Merger: GW170817 and GRB 170817A. *Astrophys. J. Lett.* **2017**, *848*, 13. [CrossRef]

30. Drout, M.R.; Piro, A.L.; Shappee, B.J.; Kilpatrick, C.D.; Simon, J.D.; Contreras, C.; Coulter, D.A.; Foley, R.J.; Siebert, M.R.; Morrell, N.; et al. Light curves of the neutron star merger GW170817/SSS17a: Implications for r-process nucleosynthesis. *Science* **2017**, *358*, 1570. [CrossRef]

31. Evans, P.A.; Cenko, S.B.; Kennea, J.A.; Emery, S.W.K.; Kuin, N.P.M.; Korobkin, O.; Wollaeger, R.T.; Fryer, C.L.; Madsen, K.K.; Harrison, F.A.; et al. Swift and NuSTAR observations of GW170817: Detection of a blue kilonova. *Science* **2017**, *358*, 1565. [CrossRef]

32. Li, L.X.; Paczyński, B. Transient Events from Neutron Star Mergers. *Astrophys. J. Lett.* **1998**, *507*, 59. [CrossRef]

33. Pian, E.; D'Avanzo, P.; Benetti, S.; Branchesi, M.; Brocato, E.; Campana, S.; Cappellaro, E.; Covino, S.; d'Elia, V.; Fynbo, J.P.U.; et al. Spectroscopic identification of r-process nucleosynthesis in a double neutron-star merger. *Nature* **2017**, *551*, 67. [CrossRef] [PubMed]

34. Ghirlanda, G.; Salafia, O.S.; Paragi, Z.; Giroletti, M.; Yang, J.; Marcote, B.; Blanchard J.; Agudo I.; An T.; Bernardini, M.G.; et al. Compact radio emission indicates a structured jet was produced by a binary neutron star merger. *Science* **2019**, *363*, 968. [CrossRef]

35. Mooley, K.P.; Deller, A.T.; Gottlieb, O.; Nakar, E.; Hallinan, G.; Bourke, S.; Frail, D.A.; Horesh, A.; Corsi, A.; Hotokezaka, K. Superluminal motion of a relativistic jet in the neutron-star merger GW170817. *Nature* **2018**, *561*, 355. [CrossRef]

36. Troja, E.; King, A.R.; O'Brien, P.T.; Lyons, N.; Cusumano, G. Different progenitors of short hard Gamma-ray bursts. *Mon. Not. R. Astron. Soc.* **2008**, *385*, L10. [CrossRef]

37. Gompertz, B.P. The Progenitors of Extended Emission Gamma-ray Bursts. Ph.D. Thesis, University of Leicester, Leicester, UK, 2015.

38. Zhang, B.; Zhang, B.B.; Liang, E.W.; Gehrels, N.; Burrows, D.N.; Mészáros, P. Making a Short Gamma-ray Burst from a Long One: Implications for the Nature of GRB 060614. *Astrophys. J.* **2007**, *655*, L25. [CrossRef]

39. Poole, T.S.; Breeveld, A.A.; Page, M.J.; Landsman, W.; Holland, S.T.; Roming, P.; Kuin, N.P.M.; Brown, P.J.; Gronwall, C.; Hunsberger, S.; et al. Photometric calibration of the Swift ultraviolet/optical telescope. *Mon. Not. R. Astron. Soc.* **2008**, *383*, 627. [CrossRef]

40. Breeveld, A.A.; Curran, P.A.; Hoversten, E.A.; Koch, S.; Landsman, W.; Marshall, F.E.; Page, M.J.; Poole, T.S.; Roming, P.; Smith, P.J.; et al. Further calibration of the Swift ultraviolet/optical telescope. *Mon. Not. R. Astron. Soc.* **2010**, *406*, 1687. [CrossRef]

41. Roming, P.W.A.; Koch, T.S.; Oates, S.R.; Porterfield, B.L.; Vanden Berk, D.E.; Boyd, P.T.; Holland, S.T.; Hoversten, E.A.; Immler, S.; Marshall, F.E.; et al. The First Swift Ultraviolet/Optical Telescope GRB Afterglow Catalog. *Astrophys. J.* **2009**, *690*, 163. [CrossRef]

42. Roming, P.W.; Koch, T.S.; Oates, S.R.; Porterfield, B.L.; Bayless, A.J.; Breeveld, A.A.; Gronwall, C.; Kuin, N.P.M.; Page, M.J.; De Pasquale, M.; et al. A Large Catalog of Homogeneous Ultra-Violet/Optical GRB Afterglows: Temporal and Spectral Evolution. *ApJS* **2017**, *228*, 13. [CrossRef]

43. Gomboc, A.; Kobayashi, S.; Mundell, C.G.; Guidorzi, C.; Melandri, A.; Steele, I.A.; Smith, R.J.; Bersier, D.; Carter, D.; Bode, M.F. Optical flashes, reverse shocks and magnetization. *AIP Conf. Proc.* **2009**, *1133*, 145.

44. Granot, J.; Sari, R. The Shape of Spectral Breaks in Gamma-ray Bur st Afterglows. *Astrophys. J.* **2002**, *568*, 820. [CrossRef]

45. GAIA Collaboration. Summary of the contents and survey properties. *Astron. Astrophys.* **2018**, *616*, 1. [CrossRef]

46. Magnier, E.A.; Schlafly, E.F.; Finkbeiner, D.P.; Tonry, J.L.; Goldman, B.; Röser, S.; Schilbach, E.; Casertano, S.; Chambers, K.C.; Flewelling, H.A.; et al. Pan-STARRS Photometric and Astrometric Calibration. *ApJS* **2020**, *251*, 6. [CrossRef]

47. The Alfred P. Sloan Foundation. 2014. Available online: https://skyserver.sdss.org/dr12/en/credits/creditshome.aspx (accessed on 30 August 2017).

48. Skrutskie, M.F.; Cutri, R.M.; Stiening, R.; Weinberg, M.D.; Schneider, S.; Carpenter, J.M.; Beichman, C.; Capps, R.; Chester, T.; Elias, J.; et al. The Two Micron All Sky Survey (2MASS). *Astrophys. J.* **2006**, *131*, 1163. [CrossRef]

49. Bertin, E.; Arnouts, S. SExtractor: Software for source extraction. *Astron. Astrophys. Supp.* **1996**, *317*, 393. [CrossRef]

50. Tody, D. The IRAF Data Reduction and Analysis System. *SPIE VI* **1986**, *627*, 733.

51. Tody, D. IRAF in the Nineties. *ASPC* **1993**, *52*, 173.

52. Blanchard, P.K.; Berger, E.; Fong, W.F. The Offset and Host Light Distributions of Long Gamma-ray Bursts: A New View From HST Observations of Swift Bursts. *Astrophys. J.* **2016**, *817*, 144. [CrossRef]

53. Nugent, A.E.; Fong, W.F.; Dong, Y.; Leja, J.; Berger, E.; Zevin, M.; Chornock, R.; Cobb, B.E.; Kelley, L.Z.; Kilpatrick, C.D.; et al. Short GRB Host Galaxies. II. A Legacy Sample of Redshifts, Stellar Population Properties, and Implications for Their Neutron Star Merger Origins. *Astrophys. J.* **2022**, *940*, 57. [CrossRef]

54. Leja, J.; Johnson, B.D.; Conroy, C.; Van Dokkum, P.G.; Byler, N. Deriving Physical Properties from Broadband Photometry with PROSPECTOR: Description of the Model and a Demonstration of its Accuracy Using 129 Galaxies in the Local Universe. *Astrophys. J.* **2019**, *837*, 170. [CrossRef]

55. Leja, J.; Speagle, J.S.; Johnson, B.D.; Conroy, C.; Van Dokkum, P.; Franx, M., A New Census of the 0.2 < z < 3.0 Universe. I. The Stellar Mass Function. *Astrophys. J. Lett.* **2020**, *893*, 111.

56. Popesso, P.; Concas, A.; Cresci, G.; Belli, S.; Rodighiero, G.; Inami, H.; Dickinson, M.; Ilbert, O.; Pannella, M.; Elbaz, D. The main sequence of star-forming galaxies across cosmic times. *Mon. Not. R. Astron. Soc.* **2023**, *519*, 1526. [CrossRef]

57. Nugent, A.E.; Fong, W.F.; Castrejon, C.; Leja, J.; Zevin, M.; Ji, A.P. A Population of Short-duration Gamma-ray Bursts with Dwarf Host Galaxies. *Astrophys. J.* **2023**, arXiv:2310.12202v1.

58. Sari, R.; Piran, T.; Halpern, J.P. Jets in Gamma-ray Bursts. *Astrophys. J. Lett.* **1999**, *519*, 17. [CrossRef]

59. Racusin, J.L.; Liang, E.W.; Burrows, D.N.; Falcone, A.; Sakamoto, T.; Zhang, B.B.; Zhang, B.; Evans, P.; Osborne, J. Jet Breaks and Energetics of Swift Gamma-ray Burst X-Ray Afterglows. *Astrophys. J.* **2009**, *698*, 43. [CrossRef]

60. Nathanail, A. Binary Neutron Star and Short Gamma-ray Burst Simulations in Light of GW170817. *Galaxies* **2018**, *6*, 119. [CrossRef]

61. Watson, D.; Hansen, C.J.; Selsing, J.; Koch, A.; Malesani, D.B.; Andersen, A.C.; Fynbo, J.P.; Arcones, A.; Bauswein, A.; Covino, S.; et al. Identification of strontium in the merger of two neutron stars. *Nature* **2019**, *574*, 497. [CrossRef]

62. Pian, E. Mergers of binary neutron star systems: A multi-messenger revolution. *Front. Astron. Space Sci.* **2020**, *7*, 108.

63. Levan, A.; Gompertz, B.P. JWST detection of heavy neutron capture elements in a compact object merger. *arXiv* **2023**, arXiv:2307.02098.

64. Rosswog, S.; Sollerman, J.; Feindt, U.; Goobar, A.; Korobkin, O.; Wollaeger, R.; Fremling, C.; Kasliwal, M.M. The first direct double neutron star merger detection: Implications for cosmic nucleosynthesis. *Astron. Astrophys.* **2018**, *615*, 132. [CrossRef]

65. Troja, E.; Piro, L.; van Eerten, H.; Wollaeger, R.T.; Im, M.; Fox, O.D.; Butler, N.R.; Cenko, S.B.; Sakamoto, T.; Fryer, C.L.; et al. The X-ray counterpart to the gravitational-wave event GW170817. *Nature* **2017**, *551*, 71. [CrossRef]

66. Hallinan, G.; Corsi, A.; Mooley, K.P.; Hotokezaka, K.; Nakar, E.; Kasliwal, M.M.; Kaplan, D.L.; Frail, D.A.; Myers S.T.; Murphy T.; et al. A radio counterpart to a neutron star merger. *Science* **2017**, *358*, 1579. [CrossRef] [PubMed]

67. Troja, E.; Piro, L.; Ryan, G.; van Eerten, H.; Ricci, R.; Wieringa, M.H.; Lotti, S.; Sakamoto, T.; Cenko, S.B. The outflow structure of GW170817 from late-time broad-band observations. *Mon. Not. R. Astron. Soc.* **2018**, *478L*, 18. [CrossRef]

68. Layman, J.D.; Lamb, G.P.; Levan, A.J.; Mandel, I.; Tanvir, N.R.; Kobayashi, S.; Gompertz, B.; Hjorth J.; Fruchter, A.S.; Kangas, T.; et al. The optical afterglow of the short Gamma-ray burst associated with GW170817. *NatAs* **2018**, *2*, 751. [CrossRef]

69. Margutti, R.; Alexander, K.D.; Xie, X.; Sironi, L.; Metzger, B.D.; Kathirgamaraju, A.; Fong, W.; Blanchard, P.K.; Berger, E.; MacFadyen, A.; et al. The Binary Neutron Star Event LIGO/Virgo GW170817 160 Days after Merger: Synchrotron Emission across the Electromagnetic Spectrum. *Astrophys. J. Lett.* **2018**, *856*, 18. [CrossRef]

70. Troja, E.; Van Eerten, H.; Ryan, G.; Ricci, R.; Burgess, J.M.; Wieringa, M.; Piro, L.; Cenko, S.B.; Sakamoto, T. A year in the life of GW 170817: The rise and fall of a structured jet from a binary neutron star merger. *Mon. Not. R. Astron. Soc.* **2019**, *489*, 1919.

71. Makhathini, S.; Mooley, K.P.; Brightman, M.; Hotokezaka, K.; Nayana, A.J.; Intema, H.T.; Dobie, D.; Lenc, E.; Perley, D.A.; Fremling, C.; et al. The Panchromatic Afterglow of GW170817: The Full Uniform Data Set, Modeling, Comparison with Previous Results, and Implications. *Astrophys. J.* **2021**, *992*, 154. [CrossRef]

72. Granot, J.; Panaitescu, A.; Kumar, P.; Woosley, S.E. Off-Axis Afterglow Emission from Jetted Gamma-ray Bursts. *Astrophys. J. Lett.* **2002**, *570*, 61. [CrossRef]

73. Foreman-Mackey, D.; Conley, A.; Meierjurgen F.W.; Hogg, D.W.; Lang, D.; Marshall, P.; Price-Whelan, A.; Sanders, J.; Zuntz, J. emcee: The MCMC Hammer. *Publ. Astron. Soc. Pac.* **2013**, *125*, 306. [CrossRef]

74. Lazzati, D. Short Duration Gamma-ray Bursts and Their Outflows in Light of GW170817. *Front. Astron. Space Sci.* **2020**, *7*, 78L. [CrossRef]

75. Troja, E. Eighteen Years of Kilonova Discoveries with Swift. *Universe* **2023**, *9*, 245. [CrossRef]

76. Rossi, A.; Stratta, G.; Maiorano, E.; Spighi, D.; Masetti, N.; Palazzi, E.; Gardini, A.; Melandri, A.; Nicastro, L.; Pian, E. A comparison between short GRB afterglows and kilonova AT2017gfo: Shedding light on kilonovae properties. *Mon. Not. R. Astron. Soc.* **2020**, *493*, 3379. [CrossRef]

77. Gompertz, B.P.; Levan, A.J.; Tanvir, N.R.; Hjorth, J.; Covino, S.; Evans, P.A.; Fruchter, A.S.; González-Fernández, C.; Jin, Z.P.; Lyman, J.D.; et al. The Diversity of Kilonova Emission in Short Gamma-ray Bursts. *Astrophys. J.* **2018**, *860*, 62. [CrossRef]

78. Jin, Z.-P.; Kenta, H.; Xiang, L.; Masaomi, T.; Paolo, D'A.; Fan, Y.Z.; Stefano C.; Wei, D.M.; Tsvi, P. The Macronova in GRB 050709 and the GRB-macronova connection. *Nat. Comm.* **2016**, *7*, 12898. [CrossRef] [PubMed]

79. Troja, E.; Castro-Tirado, A.J.; Becerra, G.J.; Hu, Y.; Ryan, G.S.; Cenko, S.B.; Ricci, R.; Novara, G.; Sánchez-Rámirez, R.; Acosta-Pulido, J.A.; et al. Erratum: The afterglow and kilonova of the short GRB 160821B. *Mon. Not. R. Astron. Soc.* **2019**, *490*, 4367. [CrossRef]

80. Mangano, V.; Holland, S.T.; Malesani, D.; Troja, E.; Chincarini, G.; Zhang, B.; La Parola, V.; Brown, P.J.; Burrows, D.N.; Campana, S.; et al. Swift observations of GRB 060614: An anomalous burst with a well behaved afterglow. *Astron. Astrophys.* **2007**, *470*, 105. [CrossRef]

81. Yang, B.; Jin, Z.P.; Li, X.; Stefano, C.; Zheng, X.Z.; Kenta, H.; Fan, Y.Z.; Tsvi, P.; Wei, D.M. A possible macronova in the late afterglow of the long-short burst GRB 060614. *Nat. Comm.* **2015**, *6*, 7323. [CrossRef]

82. Jin, Z.-P.; Li, X.; Cano, Z.; Covino, S.; Fan, Y.-Z.; Wei, D.-M. The Light Curve of the Macronova Associated with the Long-Short Burst GRB 060614. *Astrophys. J. Lett.* **2015**, *811*, 22 [CrossRef]

83. Zhang, B.; Fan, Y.Z.; Dyks, J.; Kobayashi, S.; Mészáros, P.; Burrows, D.N.; Nousek, J.A.; Gehrels, N. Physical Processes Shaping Gamma-ray Burst X-ray Afterglow Light Curves: Theoretical Implications from the Swift X-ray Telescope Observations. *Astrophys. J.* **2006**, *642*, 354. [CrossRef]

84. Sari, R.; Mészáros, P. Impulsive and Varying Injection in Gamma-ray Burst Afterglows. *Astrophys. J.* **2000**, *535*, L33. [CrossRef] [PubMed]

85. De Pasquale, M.; Schady, P.; Kuin, N.P.M.; Page, M.J.; Curran, P.A.; Zane, S.; Oates, S.R.; Holland, S.T.; Breeveld, A.A.; Hoversten, E.A.; et al. Swift and Fermi Observations of the Early Afterglow of the Short Gamma-ray Burst 090510. *Astrophys. J. Lett.* **2010**, *709*, 146. [CrossRef]

86. Abdo, A.A.; Ackermann, M.; Asano, K.; Atwood, W.B.; Axelsson, M.; Baldini, L.; Ballet, J.; Band, D.L.; Barbiellini, G.; Bastieri, D.; et al. Fermi Observations of High-energy Gamma-ray Emission from GRB 080825C. *Astrophys. J.* **2009**, *707*, 580. [CrossRef]

87. Evans, P.A.; Beardmore, A.P.; Page, K.L.; Tyler, L.G.; Osborne, J.P.; Goad, M.R.; O'Brien, P.T.; Vetere, L.; Racusin, J.; Morris, D.; et al. An online repository of Swift/XRT light curves of γ-ray bursts. *Astron. Astrophys.* **2007**, *469*, 379. [CrossRef]

88. Evans, P.A.; Beardmore, A.P.; Page, K.L.; Osborne, J.P.; O'Brien, P.T.; Willingale, R.; Starling, R.L.C.; Burrows, D.N.; Godet, O.; Vetere, L.; et al. Methods and results of an automatic analysis of a complete sample of Swift-XRT observations of GRBs. *Astron. Astrophys.* **2009**, *397*, 1177.

89. Oates, S.R.; Page, M.J.; Schady, P.; De Pasquale, M.; Koch, T.S.; Breeveld, A.A.; Brown, P.J.; Chester, M.M.; Holland, S.T.; Hoversten, E.A.; et al. A statistical study of Gamma-ray burst afterglows measured by the Swift Ultraviolet Optical Telescope. *Mon. Not. R. Astron. Soc.* **2009**, *395*, 490. [CrossRef]

90. Panaitescu, A.; Kumar, P. Analytic Light Curves of Gamma-ray Burst Afterglows: Homogeneous versus Wind External Media. *Mon. Not. R. Astron. Soc.* **2020**, *543*, 66. [CrossRef]

91. Sari, R. Hydrodynamics of Gamma-ray Burst Afterglow. *Astrophys. J.* **1997**, *489*, L37. [CrossRef]

92. Guetta, D.; Granot, J. High-Energy Emission from the Prompt Gamma-ray Burst. *Astrophys. J. Lett.* **2003**, *585*, 885. [CrossRef]

93. Nicuesa-Guelbenzu, A.; Klose, S.; Krühler, T.; Greiner, J.; Rossi, A.; Kann, D.A.; Olivares, F.; Rau, A.; Afonso, P.M.J.; Elliott, J.; et al. The late-time afterglow of the extremely energetic short burst GRB 090510 revisited. *Astron. Astrophys.* **2012**, *538*, 7. [CrossRef]

94. Rosswog, S.; Ramirez-Ruiz, E.; Davies, M.B. High-resolution calculation of merging neutron stars—III. Gamma-ray bursts. *Mon. Not. R. Astron. Soc.* **2003**, *345*, 1077. [CrossRef]

95. Blandford, R.D.; Znajek, R.L. Electromagnetic extraction of energy from Kerr black holes. *Mon. Not. R. Astron. Soc.* **1977**, *179*, 433. [CrossRef]

96. Zhang, B.; Yan, H. The Internal-collision-induced Magnetic Reconnection and Turbulence (ICMART) Model of Gamma-ray Bursts. *Astrophys. J.* **2011**, *726*, 90. [CrossRef]

97. Evans, P.A.; Osborne, J.P.; Kennea, J.A.; Campana, S.; O'Brien, P.T.; Tanvir, N.R.; Racusin, J.L.; Burrows, D.N.; Cenko, S.B.; Gehrels, N. Optimization of the Swift X-ray follow-up of Advanced LIGO and Virgo gravitational wave triggers in 2015–16. *Mon. Not. R. Astron. Soc.* **2016**, *455*, 1522. [CrossRef]

98. Abadie, J.; Abbott, B.P.; Abbott, R.; Abernathy, M.; Accadia, T.; Acernese, F.; Adams, C.; Adhikari, R.; Ajith, P.; Allen, B.; et al. TOPICAL REVIEW: Predictions for the rates of compact binary coalescences observable by ground-based gravitational-wave detectors. *CQGra* **2010**, *27*, 173001. [CrossRef]

99. Nakar, E.; Gal-Yam, A.; Fox, D.B. The Local Rate and the Progenitor Lifetimes of Short-Hard Gamma-ray Bursts: Synthesis and Predictions for the Laser Interferometer Gravitational-Wave Observatory. *Astrophys. J.* **2006**, *650*, 281. [CrossRef]

100. Zhang, G.Q.; Wang, F.Y. The Formation Rate of Short Gamma-ray Bursts and Gravitational Waves. *Astrophys. J.* **2018**, *852*, 1. [CrossRef]

101. Metzger, B.D.; Berger, E. What is the Most Promising Electromagnetic Counterpart of a Neutron Star Binary Merger? *Astrophys. J.* **2012**, *746*, 48. [CrossRef]

102. Abbott, B.P. et al. [LIGO Scientific Collaboration, Virgo Collaboration] GW170817: Observation of Gravitational Waves from a Binary Neutron Star Inspiral. *PhysRevLett* **2017**, *119*, 161101.

103. Barnes, J.; Kasen, D. Effect of a High Opacity on the Light Curves of Radioactively Powered Transients from Compact Object Mergers. *Astrophys. J.* **2013**, *775*, 18. [CrossRef]

104. Eichler, M.A. Nucleosynthesis in Explosive Environments: Neutron Star Mergers and Core-Collapse Supernovae. Ph.D. Thesis, University of Basel, Basel, Switzerland, 2017. Available online: https://edoc.unibas.ch/59530/1/Thesis_finalsubmit.pdf (accessed on 30 August 2017).

105. Gao, H.; Zhang, B.; Lü, H.J.; Li, Y. Searching for Magnetar-powered Merger-novae from Short GRBS. *Astrophys. J.* **2017**, *837*, 50. [CrossRef]

106. Dai, Z.-G.; Lu, T. Gamma-ray burst afterglows and evolution of post-burst fireballs with energy injection from strongly magnetic millisecond pulsars. *Astron. Astrophys.* **1998**, *333*, L87.

107. Rowlinson, A.; O'Brien, P.T.; Metzger, B.D.; Tanvir, N.R.; Levan, A.J. Signatures of magnetar central engines in short GRB light curves. *Mon. Not. R. Astron. Soc.* **2013**, *430*, 1061. [CrossRef]

108. Rastinejaad, J.; Gompertz, B.P.; Levan, A.J.; Fong, W.F.; Nicholl, M.; Lamb, G.P.; Malesani, D.B.; Nugent, A.E.; Oates, S.R.; Tanvir, N.R.; et al. A kilonova following a long-duration Gamma-ray burst at 350 Mpc. *Nature* **2022**, *612*, 223. [CrossRef]